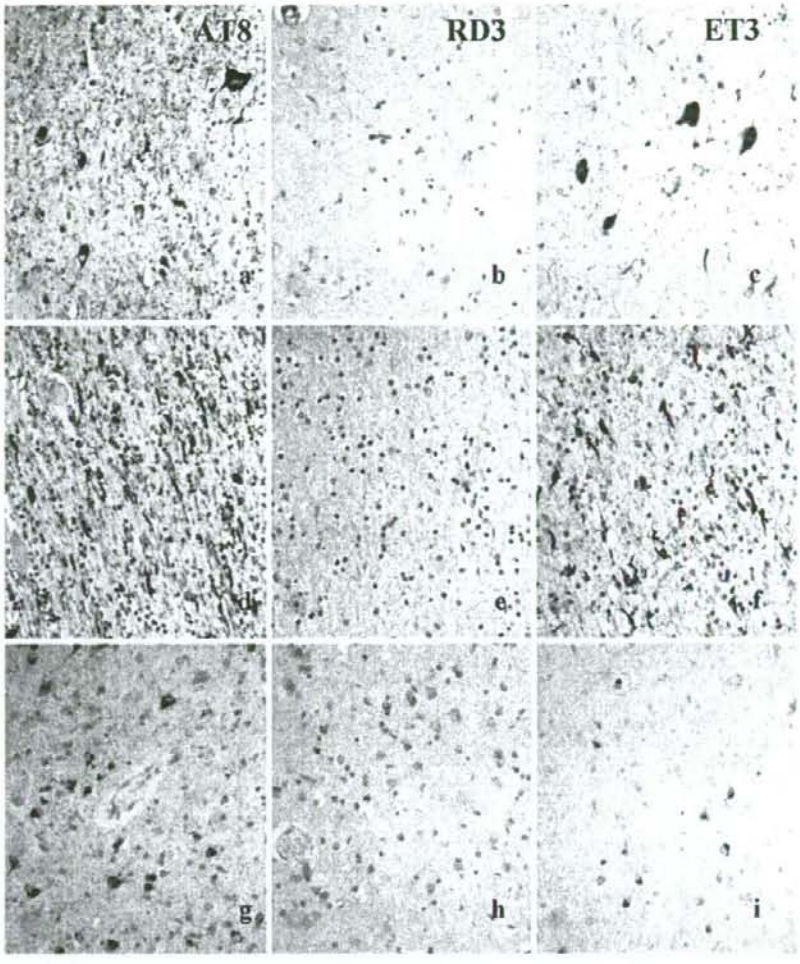

Fig. 3 Tau pathology in patients with familial FTLD. In patient #23 with *MAPT* N279K mutation (**a**–**f**), pyramidal cells of the frontal cortex are immunoreactive with AT8 (**a**) and ET3 (**c**) antibodies, but not with RD3 (**b**) antibody. Similarly, numerous glial cells within white matter of the frontal cortex contain tangles that are immunoreactive with AT8 antibody (**d**) and most of which are also reactive with ET3 antibody (**f**), but not with RD3 (**e**) antibody. In patient #25 with *MAPT* P301L mutation (**g**–**i**) neurones show amorphous tau deposits or neurofibrillary tangle-like structures that are immunoreactive with AT8 (**g**) and ET3 (**i**) antibodies, but not with RD3 antibody (**h**). In this patient numerous neuropil threads reactive only with AT8 antibody (**g**) are seen. Immunoperoxidase-haematoxylin, AT8 antibody (**a**, **d**, **g**), RD3 antibody (**b**, **e**, **h**), ET3 antibody (**c**, **f**, **i**). All 250 times microscope magnification

AT8-immunoreactive neurons were also stained with ET3 antibody, adopting a NFT-like appearance in some instances, but in others a perinuclear ring or crescent shaped structure was seen (Fig. 3i). In cases #25 and 26 none of the AT8-positive structures in nerve cells were stained with RD3 antibody (Fig. 3h), though in cases #27 and 28, respectively, rare or occasional nerve cells were RD3 reactive.

Discussion

In the present report, we have investigated by immunohistochemistry the tau isoform composition of the tau pathology present in 14 cases of sporadic FTLD and 27 cases of familial FTLD association with mutations in *MAPT* employing antibodies specific to 3R and 4R isoforms of tau.

Biochemical analysis of sarkosyl-insoluble tau extracted from brains of patients with sporadic FTLD where Pick bodies, or Pick body-like structures, are known to be present has variably shown only 3R-tau [8, 37, 54], a mixture of 3R- and 4R-tau [1, 37, 62, 66] or only 4R-tau [47, 62, 66] to be present. We find here that whenever Pick bodies are present in hippocampus and cerebral cortex in sporadic FTLD cases, these can only be detected using the antibody to 3R-tau. These findings build on an earlier report of ours [10] in which only a single case with Pick bodies was investigated and are in agreement with other immunohistochemical studies which have employed 4R-tau, but not 3R-tau, specific antibodies [1, 26]. Zhukareva and colleagues [66] investigated 14 cases of FTLD by immunohistochemistry using (different to the present study) 3R- and 4R-tau specific antibodies. In 12 of these patients and consistent with present findings, the Pick bodies were reactive only

with 3R-tau antibody. However, in seven of these cases 4R-tau species could be detected on western blot, though by immunohistochemistry this seemed to be localized in occasional cells bearing neurofibrillary tangles rather than Pick bodies and in neuropil threads [66]. Nonetheless, the other two cases in this latter study [66] displayed Pick bodies immunoreactive only to 4R-tau species and in these only 4R-tau was detected on western blot. Case #8 in the study by Zhukareva et al. [66] was case #13 in this present study. Consistent with Zhukareva et al. [66], we also found the tau pathology in this particular case reactive only with 4R-tau antibody. However, we are not convinced that these 4R-tau immunoreactive structures are indeed Pick bodies for the following reasons. First, they had a curvilinear, crescent or ring-shaped profile distinct in appearance from the rounded or oval, compact appearance associated with classic Pick bodies [28]. Second, no tau inclusions at all were present in either dentate gyrus granule cells or pyramidal cells of the hippocampus: the presence of Pick bodies in this region is pathognomic. In this present study, case #14 displayed a similar (to case #13) pattern of 4R-tau pathology. Therefore, in this present study, we find that in all cases of sporadic FTLD where unequivocal Pick bodies are present, these contain only 3R isoforms of tau. Nonetheless, it is acknowledged from the literature that there may be (rare) cases of FTLD in which the Pick bodies contain only 4R-tau isoforms [38, 66] and other cases where a few of the Pick bodies may contain 4R-tau while the great majority are only 3R-tau positive [1]. However, Pick bodies containing 4R-tau may better described as Pick-like bodies since, in at least one instance [38], electron microscopy has revealed these to be composed of parallel, long period twisted ribbon-like structures instead of the random, straight filaments typically seen in Pick bodies [28].

Consistent with these findings in sporadic FTLD, we could not detect 4R-tau within the Pick bodies of the frontal cortex of familial FTLD cases associated with *MAPT* mutations, L266V (case #15) (see also Ref. [23]), Q336R (case #36), E342V (case #37), K369I (case #38) and G389R (case #39), despite western blots showing 4R-tau species [23, 31, 43, 44] to be present in the brains of such patients (where frozen tissues were available for analysis). de Silva and co-workers reported similar findings in two other cases with *MAPT* G389R mutation [10]. Again this apparent discrepancy can be explained in terms of anatomical compartmentalization in the case of *MAPT* L266V and E342V mutations at least. In these mutations, tau-immunoreactive astrocytes are prominent and we have shown here that such cells are 4R-tau reactive and probably therefore responsible for the presence of 4R-tau isoforms on western blot. We have not been able to determine the anatomical correlates of 4R-tau isoforms seen on western blot in *MAPT* K369I and G389R mutations, though in a previous study of ours on one case with *MAPT* G389R mutation [45] 4R-tau was, on western blotting, a very minor constituent and therefore be undetectable by immunohistochemistry [10]. Similarly, Bronner et al. [4] have recently reported Pick bodies in *MAPT* G272V mutation to contain only 3R-tau isoforms on immunohistochemistry but because of rare 4R-tau containing NFT, western blotting showed a mix pattern of 3R- and 4R-tau isoforms.

Consistent with the many reports showing, by western blot, that patients with familial FTLD associated with exon 10 coding and splice site mutations contain only mutated 4R-tau isoforms [30] or selective increases in the proportion of wild-type 4R-tau [2, 6, 9, 19, 24, 25, 35, 40, 46, 60] in their brains, we found that the neuronal and glial tau pathology in *MAPT* N279K, N296H, P301L, S305S and the *MAPT* exon 10 +16 (see also Refs. [10] and [43] for exon 10 +3 mutation) mutations was exclusively associated with 4R-tau, except in two of the *MAPT* P301L mutation cases (cases #27 and 28) in whom rare 3R-tau immunoreactive cells were present and which might reflect the coincidental presence of minor Alzheimer-type pathology involving PHF, immunoreactive with both 3R- and 4R-tau antibodies because all six tau isoforms are equally represented. Some β-amyloid plaques were also present in these two *MAPT* P301L cases, again suggestive of additional Alzheimer-type pathology. Only in *MAPT* R406W mutation did we find the numerous NFT and neuropil threads [49, 63] immunoreactive with both 3R- and 4R-tau antibodies. Western blotting of the sarkosyl-insoluble tau extracted from the brains of patients with this particular mutation shows all six tau isoforms, similar to Alzheimer's disease, to occur [24, 63]. Indeed, ultrastructurally, the NFT in *MAPT* R406W mutation are in the form of paired helical filaments identical to those in AD [49]. However, it is not clear whether the same tangle in *MAPT* R406W mutation cases is both 3R- and 4R-tau immunoreactive, or whether separate populations of tangle bearing cells are involved, some containing exclusively 3R-tau, others 4R-tau, but the finding [10] in AD that NFT cells are doubly immunoreactive for 3R- and 4R-tau would make this unlikely. Notably, *MAPT* V337M mutation shares a very similar neurofibrillary pathology as *MAPT* R406Wmutation [57, 61] with all six tau isoforms being represented on western blot [57]. It might be inferred therefore that here too the tangles would be both 3R- and 4R-tau immunoreactive, though to our knowledge such investigations have not as yet been performed.

Although some studies [31, 37] have corralled cases of CBD and PSP, as tauopathies, under the umbrella of FTLD, as allowed under McKhann criteria [34], we did not include such cases within the present investigation. This was partly because we have already reported [10] that neurofibrillary tangles in PSP are stained only or mostly with antibody to 4R-tau, as is consistent with tau biochemical findings of mostly or only 4R-tau isoforms being present in sarkosyl insoluble fractions of tau [10, 37]. Furthermore, Mott et al. [37] have also shown that sarkosyl insoluble fractions of tau in CBD are likewise

composed mostly of 4R-tau and a similar pattern of 4R-tau immunoreactivity would therefore be anticipated. Indeed this was so in a single case of CBD we have so far studied (Unpublished data).

In conclusion, we have shown here that whenever classic Pick bodies are present, be these in cases of sporadic FTLD or familial cases with *MAPT* mutations (L266V, Q336R, E342V, K369I), only 3R-tau isoforms are present in such structures. The presence of 4R-tau isoforms on western blot in *MAPT* L266V and E342V mutations relates to their presence in glial cells and not Pick bodies. We have therefore not been able to confirm previous reports of the presence of 4R-tau isoforms in Pick bodies [66] and given the structural differences between these and classic Pick bodies [38], it might be better for the moment to consider the latter as Pick body-like structures pending further investigation. Neurofibrillary and glial cell tangles in cases of familial FTLD with *MAPT* exon 10 mutations (i.e., N279K, N296H, P301L, S305S and exon 10 +16 mutations) were usually or exclusively composed of 4R-tau, consistent with biochemical findings of mostly or only 4R-tau isoforms within sarkosyl-insoluble fractions from brains of such cases. The use of such tau isoform-specific antibodies may help to further refine the pathological criteria underpinning FTLD.

Acknowledgements AMS was supported by a Wolfson Scholarship and Alzheimer's Research Trust Alzheimer's Disease Research Centre Grant to DMAM. TL is supported by the Parkinson's Disease Society. This work was supported by the Reta Lila Weston Trust for Medical Research (RdS, AL, TL) and the PSP (Europe) Association (KS), which also support the Queen Square Brain Bank. The authors thank the many other people who were involved in collecting and characterising the familial FTLD cases with *MAPT* mutations and the other sporadic FTLD cases and by doing so making this multicentre collaborative study possible. The authors would also like to thank the patients and their families, without whose generous support none of this research would have been possible.

References

1. Arai T, Ikeda K, Akiyama H, Shikamoto Y, Tsuchiya K, Yagishita S, Beach T, Rogers J, Schwab C, McGeer PL (2001) Distinct isoforms of tau aggregated in neurons and glial cells in brains of patients with Pick's disease, corticobasal degeneration and progressive supranuclear palsy. Acta Neuropathol 101:167–173
2. Arima K, Kowalska A, Hasegawa M, Mukoyama M, Watanabe R, Kawai M, Takahashi K, Iwatsubo T, Tabira T, Sunohara N (2000) Two brothers with frontotemporal dementia and parkinsonism with an N279K mutation of the tau gene. Neurology 54:1787–1795
3. Bird TD, Nochlin D, Poorkaj P, Cherrier M, Kaye J, Payami H, Peskind E, Lampe TH, Nemens E, Boyer P, Schellenberg GD (1999) A clinical pathological comparison of three families with frontotemporal dementia and identical mutations in the tau gene (P301L). Brain 122:741–756
4. Bronner IF, ter Meulen BC, Azmani A, Severijnen LA, Willemsen R, Kamphorst W, Ravid R, Heutink P, van Swieten JC (2005) Hereditary Pick's disease with the G272V tau mutation shows a predominant three-repeat tau pathology. Brain 128:2645–2653
5. Bugiani O, Murrell JR, Giaccone G, Hasegawa M, Ghigo G, Tabaton M, Morbin M, Primavera A, Carella F, Solaro C, Grisoli M, Savoiardo M, Spillantini MG, Tagliavini F, Goedert M, Ghetti B (1999) Frontotemporal dementia and corticobasal degeneration in a family with a P301S mutation in tau. J Neuropathol Exp Neurol 58:667–677
6. Clark LN, Poorkaj P, Wszolek Z, Geschwind DH, Nasreddine ZS, Miller B, Li D, Payami H, Awert F, Markopoulou K, Andreadis A, D'Souza I, Lee VM, Reed L, Trojanowski JQ, Zhukareva V, Bird T, Schellenberg G, Wilhelmsen KC (1998) Pathogenic implications of mutations in the tau gene in pallidoponto-nigral degeneration and related neurodegenerative disorders linked to chromosome 17. Proc Natl Acad Sci USA 95:13103–13107
7. Constantinidis RJ, Richard J, Tissot R (1974) Pick's disease: histological and clinical correlations. Eur Neurol 11:208–217
8. Delacourte A, Sergeant N, Wattez A, Gauvreau D, Robitaille Y (1998) Vulnerable neuronal subsets in Alzheimer's and Pick's disease are distinguished by their tau isoform distribution and phosphorylation. Ann Neurol 43:193–204
9. Delisle MB, Murrell JR, Richardson R, Trofatter JA, Rascol O, Soulages X, Mohr M, Calvas P, Ghetti B (1999) A mutation at codon 279 (N279K) in exon 10 of the tau gene causes a tauopathy with dementia and supranuclear palsy. Acta Neuropathol 98:62–77
10. de Silva R, Lashley T, Gibb G, Hope A, Reid A, Bandopadhyay R, Utton M, Strand C, Jowett T, Khan N, Anderton B, Wood N, Holton J, Revesz T, Lees A (2003) Pathological inclusion bodies in tauopathies contain distinct complements of tau with three or four microtubule-binding repeat domains as demonstrated by new specific monoclonal antibodies. Neuropathol Appl Neurobiol 29:288–302
11. D'Souza I, Poorkaj P, Hong M, Nochlin D, Lee VM, Bird TD, Schellenberg GD (1999) Missense and silent tau gene mutations cause frontotemporal dementia with parkinsonism-chromosome 17 type, by affecting multiple alternative RNA splicing regulatory elements. Proc Natl Acad Sci USA 96:5598–5603
12. Foster NL, Wilhelmsen K, Sima AA, Jones MZ, D'Amato CJ, Gilman S (1997) Frontotemporal dementia and parkinsonism linked to chromosome 17: a consensus conference. Ann Neurol 41:706–715
13. Fujino Y, Wang DS, Thomas N, Espinoza M, Davies P, Dickson DW (2005) Increased frequency of argyrophilic grain disease in Alzheimer disease with 4R tau-specific immunohistochemistry. J Neuropathol Exp Neurol 64:209–214
14. Ghetti B, Murrell JR, Zolo P, Spillantini MG, Goedert M (2000) Progress in hereditary tauopathies: a mutation in the tau gene (G389R) causes a Pick disease-like syndrome. Ann N Y Acad Sci 920:52–62
15. Goedert M (2005) Tau gene mutations and their effects. Mov Disord 20(Suppl 12):S45–S52
16. Goedert M, Jakes R, Crowther RA, Six J, Lubke U, Vandermeeren M, Cras P, Trojanowski JQ, Lee VM (1993) The abnormal phosphorylation of tau protein at Ser-202 in Alzheimer disease recapitulates phosphorylation during development. Proc Natl Acad Sci USA 90:5066–5070
17. Goedert M, Spillantini MG, Crowther RA, Chen SG, Parchi P, Tabaton M, Lanska DJ, Markesbery WR, Wilhelmsen KC, Dickson DW, Petersen PB, Gambetti P (1999). Tau gene mutation in familial progressive subcortical gliosis. Nat Med 5:454–457
18. Grover A, DeTure M, Yen SH, Hutton M (2002) Effects on splicing and protein function of three mutations in codon N296 of tau in vitro. Neurosci Lett 323:33–36
19. Halliday GM, Song YJC, Creasey H, Morris JG, Brooks WS, Kril JJ (2006) Neuropathology in the S305S tau gene mutation. Brain (in press)
20. Hasegawa M, Smith MJ, Iijima M, Tabira T, Goedert M (1999) FTDP-17 mutations N279K and S305N in tau produce increased splicing of exon 10. FEBS Lett 443:93–96
21. Hayashi S, Toyoshima Y, Hasegawa M, Umeda Y, Wakabayashi K, Tokiguchi S, Iwatsubo T, Takahashi H (2002)

Late-onset frontotemporal dementia with a novel exon 1 (Arg5His) tau gene mutation. Ann Neurol 51:525–530
22. Hodges JR, Davies RR, Xuereb JH, Casey B, Broe M, Bak TH, Kril JJ, Halliday GM (2004) Clinicopathological correlates in frontotemporal dementia. Ann Neurol 56:399–406
23. Hogg M, Grujic ZM, Baker M, Demirci S, Guillozet AL, Sweet AP, Herzog LL, Weintraub S, Mesulam MM, LaPointe NE, Gamblin TC, Berry RW, Binder LI, de Silva R, Lees A, Espinoza M, Davies P, Grover A, Sahara N, Ishizawa T, Dickson D, Yen SH, Hutton M, Bigio EH (2003) The L266V tau mutation is associated with frontotemporal dementia and Pick-like 3R and 4R tauopathy. Acta Neuropathol 106:323–336
24. Hutton M, Lendon CL, Rizzu P, Baker M, Froelich S, Houlden H, Pickering-Brown S, Chakraverty S, Isaacs A, Grover A, Hackett J, Adamson J, Lincoln S, Dickson D, Davies P, Petersen RC, Stevens M, de Graaff E, Wauters E, van Baren J, Hillebrand M, Joosse M, Kwon MJ, Nowotny P, Che LK, Norton J, Morris JC, Reed LA, Trojanowski JQ, Basun H, Lannfelt L, Neystat M, Fahn S, Dark F, Tannenberg T, Dodd PR, Hayward N, Kwok JBJ, Schofield PR, Andreadis A, Snowden J, Craufurd D, Neary D, Owen F, Oostra BA, Hardy J, Goate A, van Swieten J, Mann D, Lynch T, Heutink P (1998) Association of missense and 5'-splice-site mutations in tau with the inherited dementia FTDP-17. Nature 393:702–705
25. Iseki E, Matsumura T, Marui W, Hino H, Odawara T, Sugiyama N, Suzuki K, Sawada H, Arai T, Kosaka K (2001) Familial frontotemporal dementia and parkinsonism with a novel N296H mutation in exon 10 of the tau gene and a widespread tau accumulation in the glial cells. Acta Neuropathol 102:285–292
26. Ishizawa K, Ksiezak-Reding H, Davies P, Delacourte A, Tiseo P, Yen S-H, Dickson DW (2000) A double-labelling immunohistochemical study of tau exon 10 in Alzheimer's disease, progressive supranuclear palsy and Pick's disease. Acta Neuropathol 100:235–244
27. Ishizawa T, Ko LW, Cookson N, Davies P, Espinoza M, Dickson DW (2002) Selective neurofibrillary degeneration of the hippocampal CA2 sector is associated with four repeat tauopathies. J Neuropathol Exp Neurol 61:1040–1047
28. Kertesz A, McGonagle P, Blair M, Davidson W, Munoz DG (2005) The evolution and pathology of frontotemporal dementia. Brain 128:1996–2005
29. Kobayashi T, Ota S, Tanaka K, Ito Y, Hasegawa M, Umeda Y, Motoi Y, Takanashi M, Yasuhara M, Anno M, et al (2003) A novel L266V mutation of the tau gene causes frontotemporal dementia with a unique tau pathology. Ann Neurol 53:133–137
30. Lippa CF, Zhukareva V, Kawarai T, Uryu K, Shafiq M, Nee LE, Grafman J, Liang Y, St George-Hyslop PH, Trojanowski JQ, Lee VM (2000) Frontotemporal dementia with novel tau pathology and a Glu342Val tau mutation. Ann Neurol 48:850–858
31. Lipton AM, White CL III, Bigio EH (2004) Frontotemporal lobar degeneration with motor neuron disease-type inclusions predominates in 76 cases of frontotemporal degeneration. Acta Neuropathol 108:379–385
32. Mann DMA (2005) The genetics and molecular pathology of frontotemporal lobar degeneration. In: Burns A, O'Brien J, Ames D, Arnold H (eds) Dementia, 3rd edn. , London, pp 689–701
33. Mann DMA, South PW, Snowden JS, Neary D (1993) Dementia of frontal lobe type: neuropathology and immunohistochemistry. J Neurol Neurosur Ps 56:605–614
34. McKhann GM, Albert MS, Grossman M, Miller B, Dickson D, Trojanowski JQ (2001) Workgroup on Frontotemporal dementia and Picks disease; Clinical and pathological diagnosis of frontotemporal dementia: report of the workgroup on Frontotemporal dementia and Picks disease. Arch Neurol 59:1203–1204
35. Mirra SS, Murrell JR, Gearing M, Spillantini MG, Goedert M, Crowther RA, Levey AI, Jones R, Green J, Shoffner JM, Wainer BH, Schmidt ML, Trojanowski JQ, Ghetti B (1999) Tau pathology in a family with dementia and a P301L mutation in tau. J Neuropathol Exp Neurol 58:335–345
36. Miyasaka T, Morishima-Kawashima M, Ravid R, Kamphorst W, Nagashima K, Ihara Y (2001) Selective deposition of mutant tau in the FTDP-17 brain affected by the P301L mutation. J Neuropathol Exp Neurol 60:872–884
37. Motoi Y, Iwamoto H, Itaya M, Kobayashi T, Hasegawa M, Yasuda M, Mizuno Y, Mori H (2005) Four-repeat tau positive Pick body-like inclusions are distinct from classic Pick bodies. Acta Neuropathol 110:431–433
38. Mott RT, Dickson DW, Trojanowski JQ, Zhukareva V, Lee VM, Forman M, van Deerlin V, Ervin JF, Wang DS, Schmechel DE, Hulette CM (2005) Neuropathologic, biochemical, and molecular characterization of the frontotemporal dementias. J Neuropathol Exp Neurol 64:420–428
39. Murrell JR, Spillantini MG, Zolo P, Guazzelli M, Smith MJ, Hasegawa M, Redi F, Crowther RA, Pietrini P, Ghetti B, Goedert M (1999) Tau gene mutation G389R causes a tauopathy with abundant pick body-like inclusions and axonal deposits. J Neuropathol Exp Neurol 58:1207–1226
40. Nasreddine ZS, Loginov M, Clark LN, Lamarche J, Miller BL, Lamontagne A, Zhukareva V, Lee VM, Wilhelmsen KC, Geschwind DH (1999) From genotype to phenotype: a clinical pathological, and biochemical investigation of frontotemporal dementia and parkinsonism (FTDP-17) caused by the P301L tau mutation. Ann Neurol 45:704–715
41. Neary D, Snowden JS, Mann DMA (2005) Frontotemporal dementia. Lancet Neurol 4:771–780
42. Neumann M, Schulz-Schaeffer W, Crowther RA, Smith MJ, Spillantini MG, Goedert M, Kretzschmar HA (2001) Pick's disease associated with the novel Tau gene mutation K369I. Ann Neurol 50:503–513
43. Neumann M, Mittelbronn M, Simon P, Vanmassenhove B, de Silva R, Lees A, Klapp J, Meyermann R, Kretzschmar HA (2005) A new family with frontotemporal dementia with intronic 10+3 splice site mutation in the tau gene: neuropathology and molecular effects. Neuropathol Appl Neurobiol 31:362–373
44. Papasozomenos SC (1989) Tau protein immunoreactivity in dementia of the Alzheimer type: II. Electron microscopy and pathogenetic implications. Effects of fixation on the morphology of the Alzheimer's abnormal filaments. Lab Invest 60:375–389
45. Pickering-Brown SM, Baker M, Yen S-H, Liu W-K, Hasegawa M, Cairns NJ, Lantos PL, Rossor M, Iwatsubo T, Davies Y, Allsop D, Furlong R, Owen F, Hardy J, Mann DMA, Hutton M (2000) Pick's disease is associated with mutations in the tau gene. Ann Neurol 48:859–867
46. Pickering-Brown SM, Richardson AM, Snowden JS, McDonagh AM, Burns A, Braude W, Baker M, Liu WK, Yen SH, Hardy J, Hutton M, Davies Y, Allsop D, Craufurd D, Neary D, Mann DMA (2002) Inherited frontotemporal dementia in nine British families associated with intronic mutations in the tau gene. Brain 125:732–751
47. Pickering-Brown SM, Baker M, Nonaka T, Ikeda K, Sharma S, MacKenzie J, Simpson SA, Moore JW, Snowden JS, de Silva R, Revesz T, Hasegawa M, Hutton M, Mann DM (2004) Frontotemporal dementia with Pick-type histology associated with Q336R mutation in the tau gene. Brain 127:1415–1426
48. Poorkaj P, Bird TD, Wijsman E, Nemens E, Garruto RM, Anderson L, Wiederholt WC, Raskind M, Schellenberg GD (1998) Tau is a candidate gene for chromosome 17 frontotemporal dementia. Ann Neurol 43:815–825
49. Reed LA, Grabowski TJ, Schmidt ML (1997) Autosomal dominant dementia with widespread neurofibrillary tangles. Ann Neurol 42:564–572

50. Rizzini C, Goedert M, Hodges JR, Smith MJ, Jakes R, Hills R, Xuereb JH, Crowther RA, Spillantini MG (2000) Tau gene mutation K257T causes a tauopathy similar to Pick's disease. J Neuropathol Exp Neurol 59:990–1001
51. Rizzu P, van Swieten JC, Joosse M, Hasegawa M, Stevens M, Tibben A, Niermeijer MF, Hillebrand M, Ravid R, Oostra BA, Goedert M, van Duijn CM, Heutink P (1999) High prevalence of mutations in the microtubule-associated protein tau in a population study of frontotemporal dementia in the Netherlands. Am J Hum Genet 64:414–421
52. Rosso SM, van Herpen E, Deelen W, Kamphorst W, Severijnen LA, Willemsen R, Ravid R, Niermeijer MF, Dooijes D, Smith MJ, Goedert M, Heutink P, van Swieten JC (2002) A novel tau mutation, S320F, causes a tauopathy with inclusions similar to those in Pick's disease. Ann Neurol 51:373–376
53. Rosso SM, Landweer EJ, Houterman M, Donker Kaat L, van Duijn CM, van Swieten JC (2003) Medical and environmental risk factors for sporadic frontotemporal dementia: a retrospective case-control study. J Neurol Neurosur Ps 74:1574–1576
54. Sergeant N, Wattez A, Delacourte A (1999) Neurofibrillary degeneration in progressive supranuclear palsy and corticobasal degeneration: tau pathologies with exclusively exon 10 isoforms. J Neurochem 72:1243–1249
55. Shi J, Shaw CL, Du Plessis D, Richardson AMT, Bailey K, Julien C, Neary D, Snowden JS, Mann DMA (2005) Histopathological changes underlying frontotemporal lobar degeneration with clinicopathological correlation. Acta Neuropathol 110:501–512
56. Snowden JS, Neary D, Mann DMA (1996) Fronto-temporal lobar degeneration: Fronto-temporal dementia, progressive aphasia, semantic dementia. Churchill Livingstone, Edinburgh, pp 1–227
57. Spillantini MG, Crowther RA, Goedert M (1996) Comparison of the neurofibrillary pathology in Alzheimer's disease and familial presenile dementia with tangles. Acta Neuropathol 92:42–48
58. Spillantini MG, Murrell JR, Goedert M, Farlow MR, Klug A, Ghetti B (1998) Mutation in the tau gene in familial multiple system tauopathy with presenile dementia. Proc Natl Acad Sci USA 95:7737–7741
59. Spillantini MG, Yoshida H, Rizzini C, Lantos PL, Khan N, Rossor MN, Goedert M, Brown J (2000) A novel tau mutation (N296N) in familial dementia with swollen achromatic neurons and corticobasal inclusion bodies. Ann Neurol 48:939–943
60. Stanford PM, Halliday GM, Brooks WS, Kwok JB, Storey CE, Creasey H, Morris JG, Fulham MJ, Schofield PR (2000) Progressive supranuclear palsy pathology caused by a novel silent mutation in exon 10 of the tau gene: expansion of the disease phenotype caused by tau gene mutations. Brain 123:880–893
61. Sumi SM, Bird TD, Nochlin D, Raskind MA (1992) Familial presenile dementia with psychosis associated with cortical neurofibrillary tangles and degeneration of the amygdala. Neurology 42:120–127
62. Taniguchi S, McDonagh AM, Pickering-Brown SM, Umeda Y, Iwatsubo T, Hasegawa M, Mann DM (2004) The neuropathology of frontotemporal lobar degeneration with respect to the cytological and biochemical characteristics of tau protein. Neuropathol Appl Neurobiol 30:1–18
63. van Swieten JC, Stevens M, Rosso SM, Rizzu P, Joosse M, de Koning I, Kamphorst W, Ravid R, Spillantini MG, Niermeijer M, Heutink P (1999) Phenotypic variation in hereditary frontotemporal dementia with tau mutations. Ann Neurol 46:617–626
64. Wszolek ZK, Pfeiffer RF, Bhatt MH, Schelper RL, Cordes M, Snow BJ Rodnitsky RL, Wolters EC, Arwert F, Calne DB (1992) Rapidly progressive autosomal dominant parkinsonism and dementia with pallido-ponto-nigral degeneration. Ann Neurol 32:312–320
65. Zarrantz JJ, Ferrer I, Lezcano E, Forcadas MI, Eizaguirre B, Atares B, Puig B, Gomez-Esteban JC, Fernandez-Maiztegui C, Rouco I, Perez-Concha T, Fernandez M, Rodruigez O, Rodriguez-Martinez AB, Martinez de Pancorbo M, Pastor P, Perez-Tur J (2005) A novel mutation (K317M) in the MAPT gene causes FTDP and motor neuron disease. Neurology 64:1578–1585
66. Zhukareva V, Mann DMA, Uryu K, Shuck T, Shah K, Grossman M, Miller BL, Hulette CM, Feinstein S, Trojanowski JQ, Lee VM-Y (2002) Sporadic Pick's disease: a tauopathy characterised by a spectrum of gray and white matter pathological tau isoforms. Ann Neurol 51:730–739

Available online at www.sciencedirect.com
SCIENCE DIRECT
Neuroscience Letters 400 (2006) 97–100
Neuroscience Letters
www.elsevier.com/locate/neulet

Autotaxin expression is enhanced in frontal cortex of Alzheimer-type dementia patients☆☆

Ken Umemura[a,1], Nobuyuki Yamashita[a,2], Xiaonian Yu[a], Kunimasa Arima[b], Takashi Asada[c], Takao Makifuchi[d], Shigeo Murayama[e], Yuko Saito[e], Kazutomi Kanamaru[e], Yuichi Goto[a], Shinichi Kohsaka[a], Ichiro Kanazawa[a,b], Hideo Kimura[a,*]

[a] National Institute of Neuroscience, National Center of Neurology and Psychiatry, Kodaira, Tokyo, Japan
[b] National Center Hospital for Mental, Nervous, and Muscular Disorders, National Center of Neurology and Psychiatry, Kodaira, Tokyo, Japan
[c] Institute of Clinical Medicine, University of Tsukuba, Tsukuba, Japan
[d] National Saigata Hospital, Saigata, Japan
[e] Tokyo Metropolitan Institute of Gerontology, Tokyo, Japan

Received 11 January 2006; received in revised form 3 February 2006; accepted 6 February 2006

Abstract

We searched for genes differentially expressed in the frontal cortices of Alzheimer-type dementia (ATD) patients compared with those of non-ATD controls using DNA microarray and quantitative reverse transcription-polymerase chain reaction (RT-PCR) analyses. Here we show that the expression level of the autotaxin (also called lysophospholipase D or ecto-nucleotide pyrophosphatase/phosphodiesterase 2) gene was significantly greater in ATD cortices than in non-ATD cortices. In both ATD and non-ATD groups, the expression levels were greater in patients with the apoE $\varepsilon 3/\varepsilon 4$ genotype than in patients with the apoE $\varepsilon 3/\varepsilon 3$ genotype, although the differences were not statistically significant. These observations suggest that expression of the autotaxin gene and cell signaling by lysophosphatidic acid may be involved in the pathology of ATD, and that this cell signaling pathway may be a potential target of treatments for ATD.

Keywords: Alzheimer-type dementia; Microarray; Autotaxin; Brain

The frontal cortex has major roles in higher cognitive functions, and disintegration of cognition is a major behavioral symptom of Alzheimer-type dementia (ATD) as well as memory disturbance [3]. Severe atrophy is sometimes observed in the frontal cortex as well as other sites including the hippocampus and parahippocampal gyrus of ATD patients.

Genetic linkage studies of late-onset familial Alzheimer's disease (AD) showed that AD-susceptibility is linked to the apolipoprotein E (ApoE) gene located on chromosome 19 [7]. Amyloid deposits co-localize with Apo E [6] and amyloid β-protein binds to ApoE. The Apo E gene has three variants, $\varepsilon 2$, $\varepsilon 3$, and $\varepsilon 4$, and $\varepsilon 3$ is the most common allele. The frequency of the $\varepsilon 4$ allele is higher in AD patients [8], and the copy number of this allele correlates with the age of onset of AD [1]. However, the sensitivity of ATD diagnosis using only this allele as a marker was no more than 65% [4]. The present study shows that autotaxin gene expression is greatly enhanced in the brains of ATD-patients compared with those of normal individuals. Expression of this gene tends to be greater in patients with apoE $\varepsilon 3/\varepsilon 4$ than in those with apoE $\varepsilon 3/\varepsilon 3$.

We tested postmortem brains listed in Table 1. Specimen sets A, B, and C were obtained from the National Center of Neurology and Psychiatry (NCNP; Kodaira, Tokyo, Japan) and National Saigata Hospital (Oogatamachi, Niigata, Japan). Specimen set D was from The Tokyo Metropolitan Institute of Gerontology (Itabashi, Tokyo, Japan). The patients in the non-ATD group of set D did not have amyotrophic lateral sclerosis or

☆ Supplementary material: A list of the age, gender, diagnosis for Alzheimer-type dementia, apo E genotype, and logarithmic value for the relative expression level of the autotaxin gene in each subject belonging to specimen sets C and D, normalized to that of the β actin gene, determined by quantitative reverse transcription-polymerase chain reaction (RT-PCR) experiments (Excel document).

* Corresponding author. Tel.: +81 42 346 1725; fax: +81 42 346 1755.
E-mail address: kimura@ncnp.go.jp (H. Kimura).
[1] Present address: Gifu International Institute of Biotechnology Foundation, Kakamigahara, Gifu, Japan.
[2] Present address: Meiji Seika Kaisha Ltd., Yokohama, Kanagawa, Japan.

0304-3940/$ – see front matter © 2006 Elsevier Ireland Ltd. All rights reserved.
doi:10.1016/j.neulet.2006.02.008

Table 1
Sets of specimens used

		Number of cases	Age (mean ± S.D.)
Set A[a]	ATD	7(M:4,F:3)	79.6 ± 4.8
	Non-ATD (ALS)[b]	3(M:2,F:1)	77.0 ± 8.9
Set B[a]	ATD	7(M:4,F:3)	79.6 ± 4.8
	Non-ATD (ALS)[b]	5(M:4,F:1)	72.0 ± 9.5
Set C[a]	ATD	9(M:4,F:5)	77.6 ± 6.4
	Non-ATD (ALS)[b]	5(M:4,F:1)	72.0 ± 9.5
Set D[c]	ATD	7(M:7,F:0)	90.7 ± 6.2
	Non-ATD[d]	10(M:8,F:2)	74.4 ± 7.9

[a] Set A is included in set B, and set B is included in set C.
[b] Patients had amyotrophic lateral sclerosis without dementia.
[c] Originated from an institution different from sets A–C.
[d] Patients did not have amyotrophic lateral sclerosis or dementia.

dementia, and no neuropathological symptoms of ATD were observed in their specimens. Four of them had cerebral or lacunar infarct, one cerebral hemorrhage, one small metastatic tumor, and the rest were diagnosed as unremarkable. The protocols used were approved by the local ethics committee of NCNP, National Saigata Hospital, and Tokyo Metropolitan Institute of Gerontology, respectively. Informed consent was obtained from the family of each patient. The frontal lobe was sliced into several pieces, and some were snap frozen in dry ice/ethanol and stored at −80 °C for DNA microarray and quantitative RT-PCR analyses.

Total RNA was prepared from frozen human cortical tissues using TRIzol reagent (Invitrogen), followed by purification using an RNeasy kit (Qiagen, Hilden, Germany), according to the protocols recommended by the manufacturers. To avoid potential biological hazards, homogenization of the tissues was carried out within a glove box, and all apparatus and waste that became in contact with the tissues were autoclaved at 134 °C for 1 h or immersed in disinfectant overnight. Sample preparation, hybridization, data acquisition and analysis of the DNA microarray experiment were performed according to the expression analysis technical manual for the GeneChip system (Affymetrix, Santa Clara, California). Briefly, 8–10 μg of each RNA sample was used for double-stranded cDNA synthesis, then, biotinylated antisense cRNA was synthesized. The cRNA was fragmented by heating in Mg^{2+}-containing buffer before being used for hybridization to microarrays. Human Genome U95Av2 arrays (Affymetrix) targeting about 12,000 genes were used. The hybridized arrays were stained with biotinylated anti-streptavidin antibody and streptavidin-R phycoerythrin conjugate, and the signals were measured with a confocal laser scanner (GeneArray Scanner, Affymetrix). The "signal" values representing the expression level of each gene were calculated with Microarray Suite ver 5.0 software (Affymetrix), and then statistical analyses and selection of genes of interest were performed using Data Mining Tool ver 3.0 (Affymetrix) and Genespring ver 4.1.2 (Silicon Genetics, Redwood City, California) bioinformatic algorithms. RNA prepared from each cortex was analyzed independently, and the DNA microarray experiment was repeated three times to confirm the reproducibility of results for specific genes.

cDNA was synthesized from total RNA samples using Multiple Reverse Transcriptase (Applied Biosystems, Foster City, California). Quantitative PCR by the TaqMan real-time quantitative PCR technique was performed using the PRISM 7700 Sequence Detection System (Applied Biosystems), as recommended in the instruction manuals distributed by Applied Biosystems. The forward primer, reverse primer, and TaqMan probe for each gene were designed using a sequence designing software (Primer Express version 1.5, Applied Biosystems). The nucleotide sequences for the autotoxin gene were as follows: 5′-TGCCGACAAGTGTGACGG-3′ for the forward primer, 5′-CCGGTGAGGCAGGATGAA-3′ for the reverse primer, and 5′-CCTCTCTCTGTGTCCTC-3′ for the Taqman probe. The initial amount of template in the PCR reaction was calculated based on the threshold cycle of the fluorescence curve. Relative amounts of transcripts for relevant genes and the β-actin gene in each sample were determined using an appropriate sample as a standard. The obtained values were converted to common logarithms, normalized to the means for all samples tested, and calibrated by deduction of the values for β-actin gene from those for the relevant genes of each sample.

The *P*-values for the differences in paired comparisons (Fig. 1a and b) were determined by the two-tailed Mann–Whitney *U*-test. For more detailed data analyses taking influences of multiple parameters of the subjects into account, multiple linear regression analysis was employed. The *P*-values for regression coefficients for the regressors were determined by the two-tailed one sample *t*-test.

To determine genes specifically expressed in AD brains, total RNA was prepared from seven frozen cortices of ATD cases and three cortices of ALS cases without dementia ("specimen set A" in Table 1), and DNA microarray experiments (GeneChip system; Affymetrix) targeting about 12,000 known human genes were performed. In ALS without dementia, the neuropathological symptoms appear in motor neurons but not in the central nervous system. Therefore, ALS cases were used as the control for ATD in specimen set A. The experiment was repeated three times for each RNA sample to exclude experimental artifacts. Genes showing higher (76 genes) and lower (36 genes) expressions in the ATD group were selected. The resultant genes were further examined by quantitative reverse transcription-polymerase chain reaction (RT-PCR) with TaqMan chemistry using specimen set B, which includes set A (Table 1). Fourteen genes showed higher and three genes lower expressions in ATD. Since the difference in expression of these genes could reflect the difference between ATD and ALS, the resultant genes were re-evaluated using an additional specimen set, set D, along with set C, which is an expansion of sets A and B. Specimen set D was provided by an institution different from sets A–C, and the control subjects were not ALS cases. Although the differential expressions of most of these genes were not observed in set D, it was confirmed for the autotaxin gene in both set C and set D: greater expression in ATD (Fig. 1a).

Specimen set D differs from set C in: (i) ALS morbidity, (ii) considerably older average age of the ATD group than non-ATD group, and (iii) a steeper gender ratio. Therefore, correlation between age or gender, in addition to the diagnosis (ATD or non-

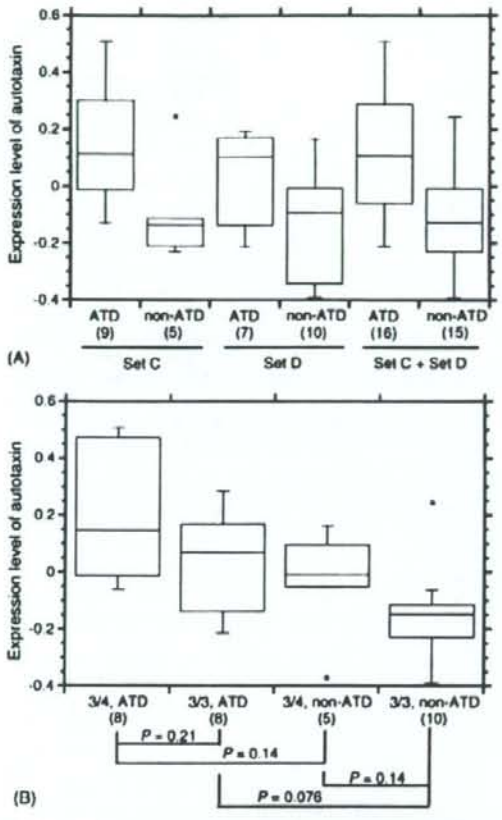

Fig. 1. Box-whisker plot representing the distribution of the expression level of the autotaxin gene. Using total RNA prepared from frozen cortices as the template, two-step quantitative RT-PCR was performed. The values were converted to common logarithms, normalized to the means for all of set C and set D samples. The normalized values for the β-actin gene were deducted from those for the autotaxin gene, and the distribution of the margin is represented. In parentheses are the numbers of samples belonging to each group. (a) Comparisons between ATD groups and non-ATD groups in specimen set C, set D, or set C plus set D. The P-value for each pair of ATD and non-ATD groups by the Mann–Whitney U-test is 0.028 for set C, 0.079 for set D, and 0.0064 for set C plus set D. (b) Two-way comparisons among ATD groups and non-ATD groups with the apoE genotype of ε3/ε4 (3/4) or ε3/ε3 (3/3) in specimen set C plus set D. The P-value for each comparison by the Mann–Whitney U-test is indicated.

ATD), and the expression of the autotaxin gene was statistically examined. When the expression data (using both specimen sets) were subjected to multiple linear regression analysis with the diagnosis, age, and gender as indicator variables, the P-value for the regression coefficient for each regressor, i.e. the diagnosis, age, and gender, in the regression model was 0.00070, 0.041, and 0.90, respectively. This indicates that diagnosis and age are probable factors linked to expression of the autotaxin gene, but gender is not. Next, the diagnosis, age, and specimen set (whether sets C or D) were introduced as indicator variables. The P-value for the regression coefficient for each of diagnosis, age, and specimen set, was 0.0025, 0.091, and 0.77, respectively. This suggests that the specimen set is not linked to expression of the autotaxin gene after the data are normalized for diagnosis and age. In other words, when the expression of the autotoxin gene is to be analyzed, specimen set C and set D may be merged as long as the diagnosis and the age are dealt with as affecting parameters. Age was slightly negatively correlated with autotaxin expression (see below). Because the average age of the ATD group was considerably older than the non-ATD group in specimen set D, for the purpose of examining the greater expression of the autotoxin gene in the ATD group, the merging of specimen set D into set C would not lead to a false positive result if age is not dealt with as an affecting parameter, though a false negative result is possible. When specimen set D was merged with set C, the significance of the differential expression of the autotoxin gene between ATD and non-ATD groups was shown more clearly even without consideration of the age ($P = 0.0064$; Fig. 1a).

For each ATD and non-ATD group in all specimens, the expression level of the autotaxin gene also appeared to be dependent on apoE genotype: a greater level in the apoE ε3/ε4 group than in the ε3/ε3 group (Fig. 1b). The differences were, however, not significant ($P = 0.21$ for the ATD group and $P = 0.14$ for the non-ATD group). At the same time, for each of the apoE ε3/ε4 and ε3/ε3 groups in all specimens, the expression level of the autotaxin gene appeared to be greater in the ATD group than in the non-ATD group ($P = 0.14$ for the apoE ε3/ε4 group and $P = 0.076$ for the ε3/ε3 group; Fig. 1b). In order to take age into account, stepwise multiple linear regression analysis was performed, with diagnosis, age, and apoE genotype being introduced as indicator variables. The P-value for the regression coefficient for each regressor, i.e. diagnosis, age, and apoE genotype, in the final regression model was 0.0013, 0.059, and 0.086, respectively. When these factors were introduced as the regressors in this order, the adjusted R^2 value at each of the three steps, which indicates the proportion of the variance of the data explicable by the regression with compensation for the number of regressors introduced, was 0.222, 0.312, and 0.362, respectively. A step-by-step increase of the adjusted R^2 value and relatively small P-values indicate that both age and apoE genotype were effective regressors. In the final regression model, the R^2 value (without adjustment for the degree of freedom) was 0.425, and the partial regression coefficients for diagnosis, age, and apoE genotype, were 0.275, −0.0077, and 0.120, respectively. They correspond to: a 1.88-fold increase in ATD subjects compared to a non-ATD subjects, a 0.84-fold decrease per 10 years of additional age, and a 1.32-fold increase in apoE ε3/ε4 subjects compared to ε3/ε3 subjects.

Autotaxin was originally isolated as an autocrine motility factor secreted by melanoma cells which promotes cell motility and metastasis [10], and was recently found to be identical to the lysophosphatidic acid (LPA)-producing enzyme, lysophospholipase D [11,12] and to NPP2, which belongs to the ectonucleotide pyrophosphatase/phosphodiesterase family [5]. LPA induces hyperphosphorylation of Tau protein [9], growth cone collapse and neurite retraction [2]. In addition, tyrosine phosphorylation of focal adhesion kinase (FAK), which is increased by amyloid β peptide [13], is modulated by LPA. These observa-

tions suggest that autotaxin may be involved in ATD pathology. Since autotaxin is a secreted enzyme, the observation that its expression level was greater in the ATD group than the non-ATD group of both apoE $\varepsilon 3/\varepsilon 4$ and $\varepsilon 3/\varepsilon 3$ in all specimens suggests the possibility that the amount of autotaxin protein or LPA in cerebro-spinal fluid can be used as a risk factor marker of ATD with any apo E genotype.

We believe that this is the first demonstration that the autotaxin gene is more strongly expressed in the brain of ATD patients. The present study suggests the possibility that the inhibition of the activity of autotaxin or signal transduction cascade for LPA in the brain might serve as a treatment or a prevention against ATD.

Acknowledgement

This work was supported by a grant from the Organization for Pharmaceutical Safety and Research.

Appendix A. Supplementary data

Supplementary data associated with this article can be found, in the online version, at doi:10.1016/j.neulet.2006.02.008.

References

[1] E.H. Corder, A.M. Saunders, W.J. Strittmatter, D.E. Schmechel, P.C. Gaskell, G.W. Small, A.D. Roses, J.L. Haines, M.A. Pericak-Vance, Gene dose of apolipoprotein E type 4 allele and the risk of Alzheimer's disease in late onset families, Science 261 (1993) 921–923.

[2] N. Fukushima, J.A. Weiner, J. Chun, Lysophosphatidic acid (LPA) is a novel extracellular regulator of cortical neuroblast morphology, Dev. Biol. 228 (2000) 6–18.

[3] M.D. Kopelman, Frontal dysfunction and memory deficits in the alcoholic Korsakoff syndrome and Alzheimer-type dementia, Brain 114 (1991) 117–137.

[4] R. Mayeux, A.M. Saunders, S. Shea, S. Mirra, D. Evans, A.D. Roses, B.T. Hyman, B. Crain, M.X. Tang, C.H. Phelps, Utility of the apolipoprotein E genotype in the diagnosis of Alzheimer's disease. Alzheimer's disease centers consortium on apolipoprotein E and Alzheimer's disease, N. Engl. J. Med. 338 (1998) 506–511.

[5] J. Murata, H.Y. Lee, T. Clair, H.C. Krutzsch, A.A. Arestad, M.E. Sobel, L.A. Liotta, M.L. Stracke, cDNA cloning of the human tumor motility-stimulating protein, autotaxin, reveals a homology with phosphodiesterases, J. Biol. Chem. 269 (1994) 30479–30484.

[6] Y. Namba, M. Tomonaga, H. Kawasaki, E. Otomo, K. Ikeda, Apolipoprotein E immunoreactivity in cerebral amyloid deposits and neurofibrillary tangles in Alzheimer's disease and kuru plaque amyloid in Creutzfeldt-Jakob disease, Brain Res. 541 (1991) 163–166.

[7] M.A. Pericak-Vance, J.L. Bebout, P.C. Gaskell Jr., L.H. Yamaoka, W.Y. Hung, M.J. Alberts, A.P. Walker, R.J. Bartlett, C.A. Haynes, K.A. Welsh, et al., Linkage studies in familial Alzheimer's disease: Evidence for chromosome 19 linkage, Am. J. Hum. Genet. 48 (1991) 1034–1050.

[8] A.M. Saunders, W.J. Strittmatter, D. Schmechel, P.H. George-Hyslop, M.A. Pericak-Vance, S.H. Joo, B.L. Rosi, J.F. Gusella, D.R. Crapper-MacLachlan, M.J. Alberts, Association of apolipoprotein E allele epsilon 4 with late-onset familial and sporadic Alzheimer's disease, Neurology 43 (1993) 1467–1472.

[9] C.L. Sayas, M.T. Moreno-Flores, J. Avila, F. Wandosell, The neurite retraction induced by lysophosphatidic acid increases Alzheimer's disease-like *Tau* phosphorylation, J. Biol. Chem. 274 (1999) 37046–37052.

[10] M.L. Stracke, H.C. Krutzsch, E.J. Unsworth, A. Arestad, V. Cioce, E. Schiffmann, L.A. Liotta, Identification, purification, and partial sequence analysis of autotaxin, a novel motility stimulating protein, J. Biol. Chem. 267 (1992) 2524–2529.

[11] A. Tokumura, E. Majima, Y. Kariya, K. Tominaga, K. Kogure, K. Yasuda, K. Fukuzawa, Identification of human plasma lysophospholipase D, a lysophosphatidic acid producing enzyme, as autotaxin, a multifunctional phosphodiesterase, J. Biol. Chem. 277 (2002) 39436–39442.

[12] M. Umezu-Goto, Y. Kishi, A. Taira, K. Hama, N. Dohmae, K. Takio, T. Yamori, G.B. Mills, K. Inoue, J. Aoki, H. Arai, Autotaxin has lysophospholipase D activity leading to tumor cell growth and motility by lysophosphatidic acid production, J. Cell Biol. 158 (2002) 227–233.

[13] C. Zhang, H.E. Qiu, G.A. Krafft, W.L. Klein, Protein kinase C and F-actin are essential for stimulation of neuronal FAK tyrosine phosphorylation by G-proteins and amyloid beta protein, FEBS Lett. 386 (1996) 185–188.

ELSEVIER

Journal of the Neurological Sciences 243 (2006) 101 – 104

Journal of the Neurological Sciences

www.elsevier.com/locate/jns

Short communication

Pathology of the sympathetic nervous system corresponding to the decreased cardiac uptake in ^{123}I-metaiodobenzylguanidine (MIBG) scintigraphy in a patient with Parkinson disease

Jun Mitsui [a], Yuko Saito [b], Toshimitsu Momose [c], Jun Shimizu [a], Noritoshi Arai [a], Junji Shibahara [d], Yoshikazu Ugawa [a], Ichiro Kanazawa [a], Shoji Tsuji [a], Shigeo Murayama [b,*]

[a] *Department of Neurology, Division of Neuroscience, Graduate School of Medicine, the University of Tokyo, Tokyo, Japan*
[b] *Department of Neuropathology, Tokyo Metropolitan Institute of Gerontology, 35-2 Sakaecho, Itabashi-ku, Tokyo 173-0015, Japan*
[c] *Department of Nuclear Medicine, the University of Tokyo, Tokyo, Japan*
[d] *Department of Human Pathology, Graduate School of Medicine, the University of Tokyo, Tokyo, Japan.*

Received 25 January 2005; received in revised form 23 November 2005; accepted 23 November 2005
Available online 27 January 2006

Abstract

Decreased cardiac uptake in ^{123}I-metaiodobenzylguanidine (MIBG) scintigraphy has been adopted as one of the most reliable diagnostic tests for Parkinson disease (PD) in Japan. To investigate the morphological basis for this finding, we performed a detailed neuropathological study of the cardiac sympathetic nervous system of a 71-year-old autopsy-proven PD patient, who presented with a marked decrease in cardiac uptake of MIBG, just 1 year prior to death. We carefully examined the intermediolateral column at several levels of the thoracic spinal cord, the sympathetic trunk and ganglia, and the nerve plexus of the anterior wall of the left ventricle and compared the findings with those of five age-matched controls. We found that the cardiac plexus was more heavily involved than the sympathetic ganglia in this patient with PD. Our study may provide further evidence that the markedly decreased cardiac uptake of MIBG observed in PD cases represents preferential involvement of the cardiac sympathetic nerve plexus in this disorder.

Keywords: Lewy body; α-synuclein; Distal axonopathy

1. Introduction

^{123}I-metaiodobenzylguanidine (MIBG) is an analogue of noradrenaline and is metabolized by noradrenergic neurons. It is therefore used as a tracer in myocardial scintigraphy for the evaluation of cardiac sympathetic innervation. Markedly decreased cardiac uptake of MIBG shown by myocardial scintigraphy is a specific finding in Parkinson disease (PD) or dementia with Lewy bodies (DLB) and is useful for the differential diagnosis of other Parkinsonian syndromes [1–4] or Alzheimer's disease [5]. This decrement has been seen even in PD patients without autonomic symptoms [2–4].

A follow-up MIBG scintigraphy study recently revealed the occurrence of a progressive decrement of MIBG uptake in cases of Yahr Stage I PD (Dr. S. Orimo, abstract of the 45th Annual Meeting of the Japanese Association of Neurology, May 2004, Tokyo) while another report showed that PD patients with normal MIBG scintigraphy have a higher incidence of mutations of the *parkin* gene (Dr. M. Yamamoto, abstract of the 45th Annual Meeting of the Japanese Association of Neurology, May 2004, Tokyo). These observations suggest that the decreased uptake of MIBG is not necessarily a finding invariably observed in patients with levodopa-responsive-Parkinsonism.

Orimo et al. reported markedly decreased tyrosine hydroxylase (TH)-immunoreactive nerve fibers in the heart of a patient with pathologically proven PD, whose

* Corresponding author. Tel.: +81 3 3964 3241; fax: +81 3 3579 4776.
E-mail address: smurayam@tmig.or.jp (S. Murayama).

0022-510X/$ - see front matter © 2005 Elsevier B.V. All rights reserved.
doi:10.1016/j.jns.2005.11.034

cardiac uptake of MIBG had been found to be severely decreased 1 year before death [6]. Amino et al. reported that not only TH-immunoreactive but also neurofilament (NF)-immunoreactive nerve fibers were markedly decreased in heart tissues from patients with pathologically proven PD [7]. Recently, Orimo et al. examined heart tissues together with sympathetic ganglia from patients with pathologically proven PD, and concluded that although sympathetic ganglia were relatively preserved, TH-immunoreactive nerve fibers were markedly decreased in heart tissues [8].

Orimo's report is the only report describing an autopsy of a PD patient who had undergone MIBG scintigraphy in situ, because the examination is usually done in the very early clinical stage of the disorder. The purpose of this study was to examine in detail the neuropathological findings of the cardiac sympathetic nervous system in a patient with PD who was examined by MIBG scintigraphy 1 year prior to death.

2. Case report and methods

2.1. Case report

A 73-year-old right-handed man visited our outpatient clinic with chief complaints of progressive gait disturbance and bradykinesia. He had been well until 9 months before this visit, at which point he noticed slowness in walking and a tendency to fall backward. His gait disturbance and bradykinesia gradually deteriorated until he required help to rise from his bed. He had a past history of exposure to the atomic bomb in Hiroshima at age 19, at which time temporarily lost his hair. He also had an 11-year history of diabetes mellitus (DM) with excellent control using glibenclamide. On neurological examination, he showed mild rigidity in his neck and four extremities, severe bradykinesia and gait of short stride with loss of arm swing. His postural reflex was also impaired but resting tremor was absent. His deep tendon reflexes were preserved and no sensory disturbances were present and he did not have any symptoms of constipation, urinary disturbances or orthostatic hypotension.

The patient's fasting blood sugar was 106 mg/dl and his hemoglobin $A1_c$ was 6.0% (normal range: 4.3–5.8%). Magnetic resonance images of the brain were unremarkable except for mild cortical atrophy, and the electrocardiogram showed unremarkable results. The coefficient of variation of the R–R interval for the electrocardiogram was 1.03% (normal range: 1.27–3.69) but the head-up tilt test showed no evidence of orthostatic hypotension. Positron emission tomography (PET) studies showed reduced ^{18}F-fluorodopa uptake with mild laterality (right>left) and increased ^{11}C-*N*-methylspiperone uptake in the striatum with mild laterality (right<left), findings which were consistent with PD.

The patient received levodopa and experienced transient amelioration, but subsequently deteriorated into a wheelchair-bound state. At age 74, he had repeated hemorrhagic episodes from diverticulitis of the colon, subsequently followed by subacutely progressive dementia with a score by Mini-Mental Stage Examination of 3, one year and six months from the onset of Parkinsonism. He unexpectedly died of massive hemorrhage 5 months later. His clinical diagnosis was PD with dementia, following the "one year rule" of the Consensus Guidelines [9]. The total clinical course was 2 years.

2.2. MIBG myocardial scintigraphy

After the patient was in the supine position for 20 min, 111 MBq of ^{123}I-MIBG (Daiichi Radioisotope Laboratories Co, Tokyo, Japan) was intravenously injected. Planar imaging and single photon emission computed tomography were performed using a triple headed gamma camera (GCA9300A, Toshiba Co, Tokyo, Japan) after 15 min (early phase) and 3 h (late phase). Photopeak energy was centered at 159 keV with a 20% window and relative organ uptake of ^{123}I-MIBG was determined by setting the region of interest on the anterior planar image. Using average counts per pixel for the heart and mediastinum, the ratio of the uptake by the heart to that by the mediastinum was calculated.

2.3. Neuropathology

A postmortem examination was performed 18 h after death. The brain and spinal cord were fixed in 20% buffered formalin for two weeks and the appropriate areas were embedded in paraffin for routine morphological examinations. To study the cardiac sympathetic innervation in detail, the intermediolateral column at several levels of the thoracic spinal cord, the sympathetic trunk and ganglia, and the nerve plexus of the anterior wall of the left ventricle were carefully examined and compared with those of five age-matched controls.

Six micron-thick sections were stained with hematoxylin and eosin by the Klüver–Barrera method. Antibodies raised against Aβ (12B2, monoclonal, aa. 11–28, IBL, Maebashi, Japan); phosphorylated τ (ptau) (AT8, Innogenetics, Temse, Belgium); phosphorylated α-synuclein (psyn) (psyn#64, monoclonal, and Pser129, polyclonal, kind gifts from Dr T. Iwatsubo), phosphorylated neurofilament (SMI31, Sternberger Immunochemicals, Bethesda, MD); HLA-DR (CD68, Dako, Glostrup, Denmark); tyrosine hydroxylase (TH, polyclonal, Calbiochem, Parmstadt, Germany); and glial fibrillary acidic protein (GFAP, polyclonal, Dako, Glostrup, Denmark) were employed. The sections were visualized with a Ventana NX20 system as previously reported [10].

The control cases died of systemic disorders that did not affect the heart.

3. Results

3.1. MIBG myocardial scintigraphy

MIBG myocardial scintigraphy revealed that the uptake ratio of the heart to that of the mediastinum was 1.58 (normal mean of 2.76) during the early phase and 1.35 (normal mean of 3.45) during the late phase.

3.2. Neuropathology

The brain weighed 1250 g and the temporal lobe was slightly atrophic. Serial coronal slices of the brain showed mild dilatation of the lateral and third ventricles and serial axial sections revealed the loss of pigmentation in the substantia nigra and locus ceruleus. Histologically, neuronal loss and gliosis were present in the substantia nigra, locus ceruleus, and basal nucleus of Meynert. Lewy bodies (LBs) were present in the substantia nigra, locus ceruleus, dorsal vagal motor nucleus, raphe nucleus, hypothalamus, basal nucleus of Meynert, amygdala, anterior cingulate gyrus, transentorhinal region and second temporal gyrus, but not present in the frontal or parietal cortex. The LB score of this case was 4, following the Consensus Guidelines for DLB [9]. Senile plaques were absent and neurofibrillary tangles were only scattered in the transentorhinal cortex (Braak Stage I).

In the sympathetic nerves innervating the heart, LBs were present in the intermediolateral column of the thoracic spinal cord and sympathetic ganglia. In contrast, LBs were completely absent in the control subjects. Multiple levels of the intermediolateral column of the thoracic spinal cord were examined with anti-phosphorylated α-synuclein antibody (psyn). Scattered psyn-immunoreactive neuronal intracytoplasmic inclusions, threads and dots were present there. Immunohistochemistry with anti-psyn antibodies showed positive axons in the thoracic ventral roots, sympathetic trunk and cardiac plexus (Fig. 1D–F) and Nageotte's residual nodules were scattered among relatively preserved sympathetic ganglia (Fig. 1A). In the cardiac plexus, total loss of TH-immunoreactivity (Fig. 1H) compared with the normal control (Fig. 1G) and a marked decrease of axons (Fig. 1C) compared with the normal control (Fig. 1B) were evident. In contrast, the dorsal root ganglia and the sural nerve, including unmyelinated fibers, were well preserved, as shown by ultrastructural studies (data not shown). The heart itself did not show any valvular, coronary or myocardial change.

4. Discussion

This study found cardiac sympathetic denervation in a patient with PD, which was well correlated with severely decreased uptake in MIBG scintigraphy.

Previous studies demonstrated that neuronal degeneration with LBs occurs in broad areas of the sympathetic nervous system, including the sympathetic ganglia and the cardiac plexus, in patients with PD [11]. In the cardiac plexus, LBs and α-synuclein positive axons [12] or

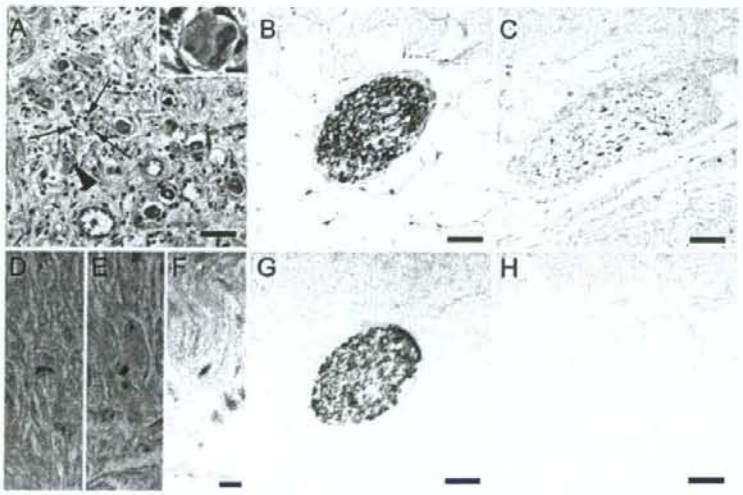

Fig. 1. Pathology of the sympathetic nervous system of a case of Parkinson disease A: a sympathetic ganglion showing a Nageotte's residual nodule (arrows) with Lewy bodies (LBs) (arrowhead) (hematoxylin and eosin staining, bar=50 μm). Inset: a typical LB in the sympathetic ganglion (bar=10 μm). B and C: unmyelinated fibers in the epicardial fatty tissue immunostained with anti-phosphorylated neurofilament antibody (SMI 31). Abundant axons from a control (B) and marked loss of axons from the case (C) (bar=50 μm). D–F: Lewy axons visualized by immunohistochemistry with anti-phosphorylated α-synuclein antibody (psyn#64) in the same fascicle as in section C (bar=10 μm). G and H: serial sections from section B (G) and C (H) immunoassayed with anti-tyrosine hydroxyls (TH) antibody. Abundant TH-immunoreactive fibers from the control (G) and total loss of immunoreactivity from the patient (H) (bar=50 μm).

markedly decreased TH-positive nerve fibers [7,8] were reported, which is consistent with our findings.

The present study found that the pathology of the sympathetic ganglia consisted of prominent α-synucleinopathy with a relatively preserved neuronal population. This was in sharp contrast with the severe axonal loss of sympathetic nerves in the cardiac muscle. Thus, LB-related α-synucleinopathy may cause distal axonopathy of the postganglionic sympathetic nerves.

It is difficult to exclude the possibility that the clinical history of DM may have made some contribution to the findings of MIBG scintigraphy and the pathology of the peripheral autonomic nervous system in this case, although the extremely low MIBG uptake and intact unmyelinated fibers in the sural nerve and dorsal root ganglia as well as pathologically unremarkable heart itself suggest that this possibility is not likely.

This study suggested that MIBG scintigraphy could be used to detect the presence of LB-related α-synucleinopathy in the cardiac sympathetic nervous system. Further prospective pathological studies on cardiac sympathetic innervation in PD or DLB patient who underwent MIBG scintigraphy should be carried out.

Acknowledgements

The authors thank Dr. Takeshi Iwatsubo (Department of Neuropathology and Neuroscience, Graduate School of Pharmaceutical Science, University of Tokyo) for kindly providing antibodies against phosphorylated α-synuclein and Ms. Azusa Uchinokura, Ms. Naoko Tokimura, Mr. Naoo Aikyo, Ms. Mieko Harada, and Ms. Nobuko Naoi for their technical support. This study was supported by Grants in Aid from the Tokyo Metropolitan Institute of Gerontology (S.M.) and from the Japanese Ministry of Education, Culture, Sports and Technology (Y.S.).

References

[1] Orimo S, Ozawa E, Nakade S, Sugimoto T, Mizusawa H. ^{123}I-metaiodobenzylguanidine myocardial scintigraphy in Parkinson's disease. J Neurol Neurosurg Psychiatry 1999;67:189–94.

[2] Taki J, Nakajima K, Kwang EH, Matsunari I, Komai K, Yoshita M, et al. Peripheral sympathetic dysfunction in patients with Parkinson's disease without autonomic failure is heart selective and disease specific. Eur J Nucl Med 2000;27:566–73.

[3] Braune S, Reinhardt M, Schnitzer R, Riedel A, Lücking CH. Cardiac uptake of [^{123}I] MIBG separates Parkinson's disease from multiple system atrophy. Neurology 1999;53:1020–5.

[4] Yoshita M. Differentiation of idiopathic Parkinson's disease from striatonigral degeneration and progressive supranuclear palsy using iodine-123meta-iodobenzylguanidine myocardial scintigraphy. J Neurol Sci 1998;155:60–7.

[5] Yoshita M, Taki J, Yamada M. A clinical role for [^{123}I] MIBG myocardial scintigraphy in the distinction between dementia of Alzheimer's-type and dementia with Lewy bodies. J Neurol Neurosurg Psychiatry 2001;71:583–8.

[6] Orimo S, Ozawa E, Oka T, Nakade S, Tsuchiya K, Yoshimoto M, et al. Different histopathology accounting for a decrease in myocardial MIBG uptake in PD and MSA. Neurology 2001;57:1140–1.

[7] Amino T, Orimo S, Itoh Y, Takahashi A, Uchichara T, Mizusawa H. Profound cardiac sympathetic denervation occurs in Parkinson disease. Brain Pathol 2005;15:29–34.

[8] Orimo S, Amino T, Itoh Y, Takahashi A, Kojo T, Uchichara T, et al. Cardiac sympathetic denervation precedes neuronal loss in the sympathetic ganglia in Lewy body disease. Acta Neuropathol 2005; 109:583–8.

[9] McKeith I.G., Galasko D, Kosaka K, Perry EK, Dickson DW, Hansen LA, et al. Consensus guidelines for the clinical and pathologic diagnosis of dementia with Lewy bodies (DLB): report of the consortium on DLB international workshop. Neurology 1996;47: 1113–24.

[10] Saito Y, Kawashima A, Ruberu NN, Fujiwara H, Koyama S, Sawabe M, et al. Accumulation of phosphorylated α-synuclein in aging human brain. J Neuropathol Exp Neurol 2003;62:644–54.

[11] Wakabayashi K, Takahashi H. Neuropathology of autonomic nervous system in Parkinson's disease. Eur Neurol 1997;38(Suppl 2):2–7.

[12] Iwanaga K, Wakabayashi K, Yoshimoto M, Tomita I, Satoh H, Takashima H, et al. Lewy body-type degeneration in cardiac plexus in Parkinson's and incidental Lewy body diseases. Neurology 1999;52: 1269–71.

Available online at www.sciencedirect.com
SCIENCE DIRECT
Neuroscience Research 54 (2006) 197–201
Neuroscience Research
www.elsevier.com/locate/neures

Increased levels of granular tau oligomers: An early sign of brain aging and Alzheimer's disease

Sumihiro Maeda [a,b], Naruhiko Sahara [a], Yuko Saito [c], Shigeo Murayama [c], Atsushi Ikai [b], Akihiko Takashima [a,*]

[a] *Lab for Alzheimer's Disease, Brain Science Institute, RIKEN, 2-1 Hirosaswa, Wako, Saitama 351-0198, Japan*
[b] *Department of Life Science, Graduate School of Bioscience and Biotechnology, Tokyo Institute of Technology, 4259 Nagatsuda, Midori-Ku, Yokohama, Kanagawa 226-8501, Japan*
[c] *Department of Neuropathology, Tokyo Metropolitan Institute of Gerontology, 35-2 Sakaecho, Itabashi-ku, Tokyo 173-0015, Japan*

Received 2 November 2005; accepted 25 November 2005
Available online 6 January 2006

Abstract

Development of neurofibrillary tangles (NFTs) is a pathological hallmark in various neurodegenerative disorders including Alzheimer's disease (AD). Recently, we identified a granular tau oligomer having a pre-filamentous structure. To determine the role of this oligomer in NFT formation, we quantified the amount of granular tau oligomer in 21 frontal cortex samples, each displaying varying degrees of Braak-staged NFT pathology. Here we report that granular tau oligomer levels in frontal cortex were significantly increased, even in brains displaying Braak-stage I neuropathology, a stage at which clinical symptoms of AD and NFTs in frontal cortex are believed to be absent. This suggests that increases in granular tau oligomer levels occur before NFTs form and before individuals manifest clinical symptoms of AD. Increased granular tau oligomer levels, therefore, may lead to NFT formation in frontal cortex, eventually leading to the development of AD. Thus, increases in granular tau oligomer levels may represent a very early sign of NFT formation and AD.

Keywords: Alzheimer's disease (AD); Tau; Atomic force microscopy (AFM); Granular tau oligomer; Braak stage; Brain aging

1. Introduction

Tau, a microtubule-associated protein, can aggregate into filamentous polymer forms (von Bergen et al., 2005). Bundled tau filaments that deposit in cells are called neurofibrillary tangles (NFTs), which commonly form in the brain during normal aging and in Alzheimer's disease (AD). In AD, NFTs and neuronal cell loss typically coincide within the same brain regions (Gomez-Isla et al., 1997). The progressively expanding anatomical distribution of NFTs reflects progressive brain dysfunction in disease, suggesting that NFT formation and neuronal cell loss may share a common mechanism (Ihara, 2001). The recent finding that patients with frontotemporal dementia and parkinsonism linked to chromosome 17 (FTDP-17) harbor tau mutations (Reed et al., 2001), strongly suggests that tau dysfunction itself can cause neurodegeneration. Indeed, the overexpression of tau in various animal models has been shown to induce neurodegeneration (Lee et al., 2001; Tanemura et al., 2001, 2002; Tatebayashi et al., 2002). However, others have observed that neuronal cell loss occurs disproportionately to the number of NFTs in AD (Gomez-Isla et al., 1997). Conversely, others have reported neuronal loss in the absence of NFTs in a tau-overexpressing *Drosophila* model (Wittmann et al., 2001), suggesting that the events that lead from tau accumulation to neurodegeneration may not involve filament formation. Recently, (Santacruz et al., 2005) reported that reducing tau overexpression in mutant tau transgenic mice decreased neuronal cell loss even though filaments continued to form, suggesting that filament formation may not be the underlying cause of neuronal cell loss. Therefore, tau may be involved in neuronal dysfunction even before NFTs are formed.

Using an in vitro tau aggregation system, we identified a granular-shaped pre-filamentous form of tau – the granular tau oligomer – composed of about 40 tau molecules (Maeda et al.,

* Corresponding author.
E-mail address: kenneth@brain.riken.go.jp (A. Takashima).

0168-0102/$ – see front matter
doi:10.1016/j.neures.2005.11.009

unpublished data). We found that increasing the concentration of granular tau oligomers in vitro causes them to convert into filaments. The breakdown of PHF into granular tau structure by continuous AFM imaging has also observed indicating that granular tau oligomer composes of filament in vivo. In the present study, to understand the relationship between the levels of granular tau oligomer and the progression of AD, we quantified the amount of granular tau oligomer in various brain samples, each histopathologically confirmed to display different Braak stages (Braak and Braak, 1991). We then compared the amounts of granular tau oligomer in each Braak-staged sample using atomic force microscopy (AFM). We found increased levels of granular tau oligomer in brain samples at Braak stage I, a stage indicative of pre-symptomatic AD. Granular tau oligomers were detected even in samples at Braak stage 0.

2. Materials and methods

2.1. Subjects

Frozen frontal cortex samples from 21 subjects, including 5 patients with AD (Murayama and Saito, 2004), were obtained from the Tokyo Metropolitan Institute of Gerontology (TMIG) (Saito et al., 2004). The brains from TMIG were staged histopathologically according to the Braak staging system (Braak and Braak, 1991).

2.2. Antibodies

Anti-paired helical filament antibody, PHF-1, was a kind gift from Dr. P. Davies (Albert Einstein College of Medicine, USA). Anti-tau antibody, JM, was raised against full-length recombinant tau (Takashima et al., 1998). Anti-tau antibody, Tau-c, was raised against tau c-terminus polypeptide (amino acids 422–438, according to the longest human tau isoform).

2.3. Purification of granular tau oligomers

Human brain samples (~12 g) were homogenized with three volumes of a buffer containing 10 mM Tris (pH 7.4), 800 mM NaCl, 1 mM EGTA, 10% sucrose, and protease inhibitors, and centrifuged at 27,000 × *g* for 20 min at 4 °C. CHAPS (Dojindo, Kumamoto, Japan) was added to the supernatant to a final concentration of 1% (w/v), then loaded into an immunoaffinity column (2 ml bed volume) containing anti-tau antibody JM. The column was washed with at least 400 ml of buffer containing 10 mM Tris (pH 7.4), 800 mM NaCl, 1 mM EGTA, and 1% CHAPS. After confirming that no aggregates remained in the wash solution, the column was eluted with 5 ml of 3M KSCN (Jicha et al., 1999). After exchanging the above buffer to a buffer containing 10 mM Tris (pH 7.4), 800 mM NaCl, and 1 mM EGTA with a NAP-10 column (Amersham Biosciences), we added *N*-lauroylsarcosine (Nacalai tesque, Kyoto, Japan) until achieving a final concentration of 1% (wt./vol.). After 2 h of incubation, 1 ml of sample was layered onto a sucrose step gradient (50, 40, 30, and 20% sucrose) and centrifuged for 2 h at 50 K rpm in a MLS50 rotor (Beckman Coulter) using an Optima MAX-E ultracentrifuge (Beckman Coulter) at 23 °C. We separated the samples into 1 ml fractions, from top to bottom (fractions 1–5), to eliminate contamination from lower fractions. We washed the bottom of tubes with buffer and saved the wash solution as fraction 6. We previously isolated granular tau oligomer from fraction 3 derived from either in vitro aggregated tau or human brain samples (Maeda et al., unpublished data). In the present study, we also found that the granular tau oligomer localized to fraction 3.

2.4. Western blot analysis

Granular tau oligomer fractions were concentrated by adding trichloroacetic acid to the fractions and setting the mixtures on ice for 2 h. The mixtures were then centrifuged at 20,000 × *g* at 4 °C, and supernatants were removed and dried in a SpeedVac Concentrator (SAVANT). Loading buffer was added to the dried granular tau oligomers, and this mixture was subjected to SDS-PAGE and subsequent immunoblotting with anti-tau antibody Tau-c.

Sarcosyl-insoluble fractions were prepared by solubilizing homogenized brain tissue (see above) in 1% sarcosyl for 2 h at 25 °C, then centrifuging at 50 K rpm in a TLA 55 rotor (Beckman Coulter) for 20 min. After removing the supernatant, loading buffer was added to the pellet, and the insoluble tau was subjected to SDS-PAGE and immunoblotting with PHF-1 antibody. Immunoreactivities were quantified with the software program Image Gauge (Fujifilm).

2.5. Atomic force microscopy

Samples were dropped onto freshly cleaved mica and left in place for 30 min prior to AFM assessment. After washing the mica with water, we examined the tau-containing samples in solution using a Nanoscope IIIa (Digital Instruments, Santa Barbara, CA, USA) set at tapping mode (Hansma et al., 1995). OMCL-TR400PSA (Olympus, Japan) was used as a cantilever. The resonant frequency was about 9 kHz.

We examined four different areas (2 μm × 2 μm each) of the mica surface covered with granular aggregates. These areas were analyzed with NIH-image 1.63 and summations of four different areas were demonstrated.

2.6. Statistical analysis

The significant difference between each Braak staging was tested with Mann–Whitney test. Data were analyzed with Prism 4 for Macintosh (Graphpad, San Diego, CA, USA).

3. Results

3.1. Purification of granular tau oligomers

We purified granular tau oligomers from human frontal cortices (Table 1) pathologically classified according to the Braak staging system (Braak and Braak, 1991) and examined the oligomers using AFM. Fig. 1 shows representative AFM images of cortex samples from a Braak-stage 0 brain (non-AD) and a Braak-stage V brain (AD). Although we detected granular tau oligomers in both of these samples, the number of oligomers in the Braak-stage V sample was much greater than that in the Braak-stage 0 sample. The size of granular tau oligomers ranged from 5 to 50 nm. The peak of granular tau oligomer was around 20 nm in diameter, which is similar with in vitro generated granular tau oligomer. And granular tau oligomers derived from in vivo and in vitro were recovered into same fraction in sucrose centrifugation, indicating the similar sedimentation coefficient between them. PHF-1 immunoreactivity and similar bands pattern with PHF-tau on immunoblotting (Fig. 2b and c, Maeda et al., unpublished data) suggested the hyperphosphorylation in granular tau oligomer.

3.2. Accumulation of granular tau oligomers during early stages of NFT formation

We quantified the number of granular tau oligomers in Braak-staged cortex samples examined with AFM using NIH-image 1.63 (Fig. 2a). In samples staged at Braak stage 0, a stage at which the brain does not contain NFTs, we detected some, albeit a few, granular tau oligomers. In samples staged at Braak stage I (i.e., neuropathology typically seen in normal brain

Table 1
Demographics and characteristics of cases

Number	Age (years)	Gender	PMT (h:min)	NFT*	Senile plaque
1	52	M	15:51	0	0
2	69	F	11:48	0	A
3	82	F	39:04	0	0
4	87	M	70:10	0	0
5	78	M	2:02	0	0
6	66	F	9:51	0	B
7	81	M	3:00	I	B
8	97	F	2:40	I	B
9	84	M	47:25	I	B
10	87	M	4:25	I	C
11	93	M	20:49	I	C
12	86	F	6:50	III	C
13	94	M	13:00	III	C
14	87	F	4:21	III	C
15	82	F	10:32	III	C
16	89	F	16:11	III	C
17	90	F	64:07	V	C
18	86	F	19:51	V	C
19	93	F	13:28	V	C
20	70	M	35:42	V	C
21	80	F	6:41	V	C

Abbreviations: PMT, postmortem time; NFT, neurofibrillary tangle; SP, senile plaque.

* NFTs and SPs were staged according to the neuropathology staging system of Braak and Braak (1991).

aging), a stage at which entorhinal cortex but not frontal cortex contains NFTs, the number of granular tau oligomers present significantly increased compared to that in the Braak-stage 0 samples ($P = 0.0173$). In samples staged at Braak stage III, a stage at which both limbic areas and entorhinal cortex contain NFTs, the number of granular tau oligomers present also significantly increased compare to that in the Braak-stage 0 samples ($P = 0.0087$). In samples staged at Braak stage V, a stage at which neocortex including frontal cortex contain NFTs, the number of granules increased again significantly compare to that in Braak-stage 0 samples ($P = 0.0087$). We observed no significant differences in the number of granular tau oligomers in stage I, III, and V samples.

We confirmed these results by using Western blotting to assess granular tau oligomer fractions and conventionally purified sarcosyl-insoluble tau fractions derived from Braak-staged frontal cortices (Fig. 2b and c, respectively). The Tau-c immunostaining intensity of tau bands derived from the granular tau oligomer fraction of Braak-stage 0 samples was faint (Fig. 2b). Nonetheless, in Braak-stage I, III, and V samples, we did detect tau smears displaying a immunostaining pattern characteristic of insoluble tau (Fig. 2b cf. PHF-1 immunostaining pattern in Fig. 2c) (Selkoe et al., 1982; Ihara et al., 1983; Greenberg and Davies, 1990). Linear regression analysis revealed a significant correlation between Tau-c immunoreactivity and the number of granular tau oligomers ($P < 0.0001$, $r^2 = 0.6336$). On the other hand, similar statistical analysis failed to reveal a correlation between PHF-1 immunoreactivity and the number of granular tau oligomers.

Taken together, these results indicate that granular tau oligomer levels begin to increase in pre-symptomatic stages of disease, suggesting that granular tau oligomers may form before NFTs are formed.

4. Discussion

4.1. Granular tau oligomer as a pre-symptomatic marker for AD

Using silver-stained human brain sections, Braak and Braak (1991) described seven stages (0–VI) of neuropathology that are now commonly used to stage the progression of neurodegenerative diseases. The Braak staging system is based on the density and distribution of agyrophilic NFTs in the brain (Braak and Braak, 1991). Stage 0 is characterized by the absence of NFTs. Stages I and II are termed transentorhinal stages, because they are characterized by the presence of NFTs in the transentorhinal region. Stages I and II are distinguished by the density of NFTs. Stages III and IV are termed limbic stages, because they are characterized by the presence of NFTs in the hippocampus as well as in the transentorhinal region. Stages V and VI are termed isocortical stages, because they are

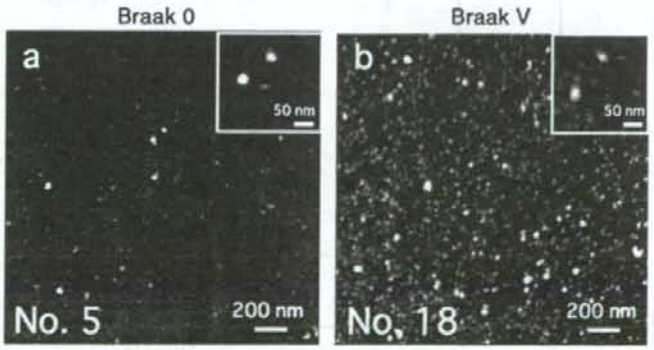

Fig. 1. Granular tau oligomers purified from human frontal cortex. Frontal cortex homogenates were fractionated with sucrose gradient centrifugation, and fractions (fraction 3) containing granular tau oligomers were examined in solution with AFM set to tapping mode. Representative data from the Braak-staged samples indicated are shown here. Insets contain high magnification AFM images of granular tau oligomers. The height range is 30 nm. The large numbers in the lower left corner of each panel correspond to the brain identification numbers in Table 1.

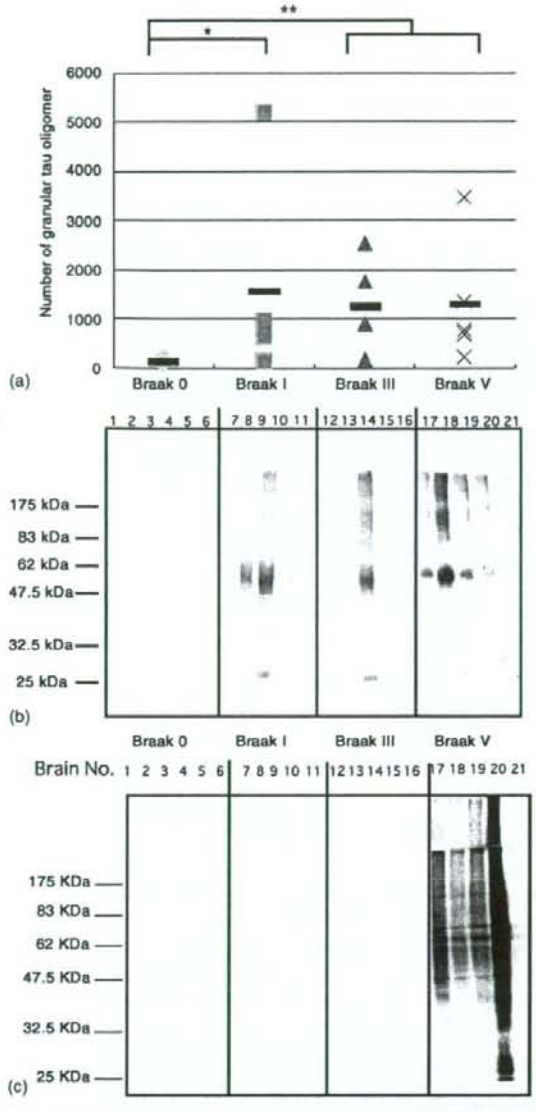

Fig. 2. The distribution of granular tau oligomers observed in different Braak stages. (a) AFM images of Braak-staged frontal cortex samples were analyzed with NIH-image 1.63, and the total number of granular aggregates in each sample were counted and graphed. $^{*}P < 0.05$, $^{**}P < 0.01$. (b) Western blots of fractions containing granular tau oligomers immunostained with Tau-c antibody. (c) Western blots of sarcosyl-insoluble fractions immunostained with PHF-1 antibody for the detection of tau filaments.

characterized by the extension of NFTs into neocortex, including frontal cortex.

The density and distribution of NFTs have been shown to increase with normal aging (Braak and Braak, 1997). Even non-AD brain specimens from individuals as old as 90 years contain NFTs. In Braak stage I, NFTs are confined within the transentorhinal region. Most of these NFTs are not accompanied by SPs, suggesting that that NFT formation occurring within the transentorhinal region is independent of SP formation, and thus may not represent a pathological process linked to AD. In line with these data is the finding that the anatomical distribution of NFTs observed in Braak stage I appears to be age dependent (Braak and Braak, 1997), which is consistent with the premise that NFT development occurs as part of normal brain aging.

We detected an increased amount of granular tau oligomers in Braak-stage I frontal cortex samples but not in Braak-stage 0 samples, suggesting that, at a time when NFTs form in the entorhinal cortex, tau dysfunction, which tau comes up from microtubule, and forms aggregate, has already started to occur in the frontal cortex, which should indicate tau dysfunction (Lu and Wood, 1993; Yoshida and Ihara, 1993). Interestingly, the level of granular tau oligomers in frontal cortex remained constant in samples staged at Braak stages II–V, even though the density of NFTs increases progressively in these stages. At this point, however, we cannot explain the incongruity between the levels of tau oligomers and NFTs. We do not know exactly how granular tau oligomers affect neuronal vulnerability.

We also investigated the relationship between granular tau oligomer formation and the density and distribution of senile plaques (SPs) (data not shown), another neuropathological hallmark of AD. We found granular tau oligomers in samples containing SPs in the neocortex (SP-stage B and C). In one Braak-stage 0 sample from an SP-stage B patient (No. 6 in Table 1), however, we did not detect a significant increase in granular tau oligomer levels, suggesting that the extent of SP pathology may not affect the formation of granular tau oligomers. Recently, Katsuno and colleagues reported that the accumulation of AB and tau occurs independently in entorhinal cortex (Katsuno et al., 2005). Therefore, the formation of granular tau oligomers may not be related to Aβ accumulation but instead may be related to some other aging-related event that occurs during Braak stage I. In later Braak stages, Aβ may accelerate the formation of granular tau oligomers that ultimately leads to NFT formation and neuronal loss. Further studies are required in order to understand the precise biochemical sequence of events underlying neuronal death, NFT formation, and granular tau oligomer formation.

References

Braak, H., Braak, E., 1991. Neuropathological stageing of Alzheimer-related changes. Acta Neuropathol. (Berl) 239–259.

Braak, H., Braak, E., 1997. Frequency of stages of Alzheimer-related lesions in different age categories. Neurobiol. Aging 351–357.

Gomez-Isla, T., Hollister, R., West, H., Mui, S., Growdon, J.H., Petersen, R.C., Parisi, J.E., Hyman, B.T., 1997. Neuronal loss correlates with but exceeds neurofibrillary tangles in Alzheimer's disease. Ann. Neurol. 17–24.

Greenberg, S.G., Davies, P., 1990. A preparation of Alzheimer paired helical filaments that displays distinct tau proteins by polyacrylamide gel electrophoresis. Proc. Natl. Acad. Sci. U.S.A. 5827–5831.

Hansma, H.G., Laney, D.E., Bezanilla, M., Sinsheimer, R.L., Hansma, P.K., 1995. Applications for atomic force microscopy of DNA. Biophys. J. 1672–1677.

Ihara, Y., 2001. PHF and PHF-like fibrils—cause or consequence? Neurobiol. Aging 123–126.

Ihara, Y., Abraham, C., Selkoe, D.J., 1983. Antibodies to paired helical filaments in Alzheimer's disease do not recognize normal brain proteins. Nature 727–730.

Jicha, G.A., O'Donnell, A., Weaver, C., Angeletti, R., Davies, P., 1999. Hierarchical phosphorylation of recombinant tau by the paired-helical filament-associated protein kinase is dependent on cyclic AMP-dependent protein kinase. J. Neurochem. 214–224.

Katsuno, T., Morishima-Kawashima, M., Saito, Y., Yamanouchi, H., Ishiura, S., Murayama, S., Ihara, Y., 2005. Independent accumulations of tau and amyloid beta-protein in the human entorhinal cortex. Neurology 687–692.

Lee, V.M., Goedert, M., Trojanowski, J.Q., 2001. Neurodegenerative tauopathies. Annu. Rev. Neurosci. 1121–1159.

Lu, Q., Wood, J.G., 1993. Functional studies of Alzheimer's disease tau protein. J. Neurosci. 508–515.

Murayama, S., Saito, Y., 2004. Neuropathological diagnostic criteria for Alzheimer's disease. Neuropathology 254–260.

Reed, L.A., Wszolek, Z.K., Hutton, M., 2001. Phenotypic correlations in FTDP-17. Neurobiol. Aging 89–107.

Saito, Y., Ruberu, N.N., Sawabe, M., Arai, T., Tanaka, N., Kakuta, Y., Yamanouchi, H., Murayama, S., 2004. Staging of argyrophilic grains: an age-associated tauopathy. J. Neuropathol. Exp. Neurol. 911–918.

Santacruz, K., Lewis, J., Spires, T., Paulson, J., Kotilinek, L., Ingelsson, M., Guimaraes, A., DeTure, M., Ramsden, M., McGowan, E., Forster, C., Yue, M., Orne, J., Janus, C., Mariash, A., Kuskowski, M., Hyman, B., Hutton, M., Ashe, K.H., 2005. Tau suppression in a neurodegenerative mouse model improves memory function. Science 476–481.

Selkoe, D.J., Ihara, Y., Salazar, F.J., 1982. Alzheimer's disease: insolubility of partially purified paired helical filaments in sodium dodecyl sulfate and urea. Science 1243–1245.

Takashima, A., Murayama, M., Murayama, O., Kohno, T., Honda, T., Yasutake, K., Nihonmatsu, N., Mercken, M., Yamaguchi, H., Sugihara, S., Wolozin, B., 1998. Presenilin 1 associates with glycogen synthase kinase-3beta and its substrate tau. Proc. Natl. Acad. Sci. U.S.A. 9637–9641.

Tanemura, K., Akagi, T., Murayama, M., Kikuchi, N., Murayama, O., Hashikawa, T., Yoshiike, Y., Park, J.M., Matsuda, K., Nakao, S., Sun, X., Sato, S., Yamaguchi, H., Takashima, A., 2001. Formation of filamentous tau aggregations in transgenic mice expressing V337M human tau. Neurobiol. Dis. 1036–1045.

Tanemura, K., Murayama, M., Akagi, T., Hashikawa, T., Tominaga, T., Ichikawa, M., Yamaguchi, H., Takashima, A., 2002. Neurodegeneration with tau accumulation in a transgenic mouse expressing V337M human tau. J. Neurosci. 133–141.

Tatebayashi, Y., Miyasaka, T., Chui, D.H., Akagi, T., Mishima, K., Iwasaki, K., Fujiwara, M., Tanemura, K., Murayama, M., Ishiguro, K., Planel, E., Sato, S., Hashikawa, T., Takashima, A., 2002. Tau filament formation and associative memory deficit in aged mice expressing mutant (R406W) human tau. Proc. Natl. Acad. Sci. U.S.A. 13896–13901.

von Bergen, M., Barghorn, S., Biernat, J., Mandelkow, E.M., Mandelkow, E., 2005. Tau aggregation is driven by a transition from random coil to beta sheet structure. Biochim. Biophys. Acta 158–166.

Wittmann, C.W., Wszolek, M.F., Shulman, J.M., Salvaterra, P.M., Lewis, J., Hutton, M., Feany, M.B., 2001. Tauopathy in *Drosophila*: neurodegeneration without neurofibrillary tangles. Science 711–714.

Yoshida, H., Ihara, Y., 1993. Tau in paired helical filaments is functionally distinct from fetal tau: assembly incompetence of paired helical filament-tau. J. Neurochem. 1183–1186.

Human Molecular Genetics, 2006, Vol. 15, No. 7 *1151–1158*
doi:10.1093/hmg/ddl030
Advance Access published on February 24, 2006

Multiple candidate gene analysis identifies α-*synuclein* as a susceptibility gene for sporadic Parkinson's disease

Ikuko Mizuta[1], Wataru Satake[1], Yuko Nakabayashi[1,2], Chiyomi Ito[1,2], Satoko Suzuki[1,2], Yoshio Momose[1,†], Yoshitaka Nagai[1], Akira Oka[3], Hidetoshi Inoko[3], Jiro Fukae[4], Yuko Saito[5,6], Motoji Sawabe[5], Shigeo Murayama[6], Mitsutoshi Yamamoto[7], Nobutaka Hattori[4], Miho Murata[8] and Tatsushi Toda[1,2,*]

[1]Division of Clinical Genetics, Department of Medical Genetics, Osaka University Graduate School of Medicine, 2-2-B9 Yamadaoka, Suita, Osaka 565-0871, Japan, [2]Core Research for Evolutional Science and Technology (CREST), Japan Science and Technology Agency, Saitama 332-0012, Japan, [3]Department of Molecular Life Science, Tokai University School of Medicine, Kanagawa 259-1193, Japan, [4]Department of Neurology, Juntendo University School of Medicine, Tokyo 113-8421, Japan, [5]Department of Pathology, Tokyo Metropolitan Geriatric Hospital, Tokyo 173-0015, Japan, [6]Department of Neuropathology, Tokyo Metropolitan Institute of Gerontology, Tokyo 173-0015, Japan, [7]Department of Neurology, Kagawa Prefectural Central Hospital, Takamatsu 760-8557, Japan and [8]Department of Neurology, Musashi Hospital, National Center of Neurology and Psychiatry, Tokyo 187-8551, Japan

Received December 22, 2005; Revised and Accepted February 15, 2006

Parkinson's disease (PD), one of the most common human neurodegenerative diseases, is characterized by the loss of dopaminergic neurons in the substantia nigra of the midbrain. PD is a complex disorder with multiple genetic and environmental factors influencing disease risk. To identify susceptible genes for sporadic PD, we performed case–control association studies of 268 single nucleotide polymorphisms (SNPs) in 121 candidate genes. In two independent case–control populations, we found that a SNP in *α-synuclein* (*SNCA*), rs7684318, showed the strongest association with PD ($P = 5.0 \times 10^{-10}$). Linkage disequilibrium (LD) analysis using 29 SNPs in a region around rs7684318 revealed that the entire *SNCA* gene lies within a single LD block ($D' > 0.9$) spanning ~120 kb. A tight LD group ($r^2 > 0.85$) of six SNPs, including rs7684318, associated most strongly with PD ($P = 2.0 \times 10^{-9}$–1.7×10^{-11}). Haplotype association analysis did not show lower *P*-values than any single SNP within this group. SNCA is a major component of Lewy bodies, the pathological hallmark of PD. Aggregation of SNCA is thought to play a crucial role in PD. *SNCA* expression levels tended to be positively correlated with the number of the associated allele in autopsied frontal cortices. These findings establish *SNCA* as a definite susceptibility gene for sporadic PD.

INTRODUCTION

Sporadic Parkinson's disease (PD) (OMIM no. 168600) is the second most common neurodegenerative disease following Alzheimer's disease. PD is late onset and progressive, affecting 1–2% of persons older than 65 years. Clinical features of PD include resting tremor, bradykinesia, rigidity and postural instability. The disease is pathologically characterized by the loss of dopaminergic neurons in the substantia nigra and the presence of intracellular inclusions known as Lewy bodies. Various medical managements are available for PD, including drugs (l-dopa, dopamine agonists, anti-cholinergic drugs, etc.) and surgery (thalamotomy, pallidotomy, deep brain stimulation, etc.) (1). These treatments improve PD symptoms, but do little to deter disease progression. Identifying risk factors for PD can be helpful in delaying disease onset and slowing its progression.

*To whom correspondence should be addressed. Tel: +81 668793380; Fax: +81 668793389; Email: toda@clgene.med.osaka-u.ac.jp
†Present address: Department of Clinical Bioinformatics, Graduate School of Medicine, University of Tokyo, Tokyo 113-8655, Japan.

PD is a complex common disease, caused by multiple genetic and environmental factors (2). The contribution of genetic factors to sporadic PD is indicated by several findings. First, ~10% of patients with PD have a positive family history (3). Secondly, a recent large-scale survey in Iceland showed that the risk ratio for PD was increased in related individuals (6.7 for siblings, 3.2 for offspring and 2.7 for nephews and nieces of patients with PD) (4). Thirdly, a twin study using [^{18}F]dopa PET showed that the concordance rate for PD, including subclinical cases, is approximately three times higher in monozygotic twins (55%) than in dizygotic twins (18%) (5).

Causal genes for Mendelian-inherited PD have been reported, including *α-synuclein* [4q21, autosomal dominant (AD)] (6), *parkin* [6q25.2–27, autosomal recessive (AR)] (7), *UCH-L1* (4p14, AD) (8), *PINK1* (1p36, AR) (9), *DJ-1* (1p36, AR) (10), *LRRK2/dardarin* (12q12, AD) (11,12) and *NR4A2/Nurr1* (2q22–23, AD) (13).

Many case–control association studies using single nucleotide polymorphisms (SNPs) in candidate genes have been reported, but few consistent findings have been obtained (2). This is due, in part, to limited numbers of available samples, target genes and/or genetic markers. Since 2001, genome-wide, non-parametric linkage analysis of PD families has revealed significant linkage in multiple chromosomal regions (14–17), leading to the identification of *tau* (18) and *FGF20* (19) as susceptibility genes.

To date, polymorphisms that influence PD as strongly as *APOE-ε4* influences Alzheimer's disease have not been identified. Through extensive candidate gene association studies, we have established *α-synuclein* (*SNCA*) as a definite susceptibility gene for sporadic PD.

RESULTS

Screening of SNPs in candidate genes for PD

We selected candidate genes from the literature describing genetic, pathological and biochemical findings in PD, as well as genes that participate in the proposed mechanisms for PD. Finally, we picked up 121 genes relevant to familial PD, Lewy bodies, dopaminergic neurons, cytokines and trophic factors, mitochondrial functions, oxidative stress, proteasome function, autophagy, endoplasmic reticulum-associated degradation (ERAD) and toxins. One to seven SNPs per gene (268 SNPs total) were selected from the dbSNP, JSNP and Celera Discovery System databases.

In the initial screen, we genotyped 190 patients and 190 controls (Supplementary Material, Table S1). To avoid false negatives, we set the α-value at 0.05 in the first screen. From 268 SNPs, 22 SNPs in 16 genes showed association with PD ($P < 0.05$) in genotype frequency, allele frequency, dominant model or recessive model. We genotyped the 22 qualifying SNPs in a replication panel of 692 patients and 748 controls and tested again for association. This independent test revealed that SNP0070 (rs7684318 C/T) was prominently associated with PD ($P = 5.0 \times 10^{-10}$ for allele frequency) (Table 1). We corrected the α-value to 0.00019 after Bonferroni's correction (tests for 268 SNPs). The remaining 21 SNPs did not show P-values lower than 0.00019 (data not shown). SNP0070 is located in intron 4 of the *α-synuclein* (*SNCA*) gene on chromosome 4q21. SNCA is a primary component of intracellular inclusions called Lewy bodies, which are considered to be the pathological hallmark of PD (20). Aggregation of SNCA is thought to play a crucial role in the pathogenesis of PD (21). The allele C frequency of SNP0070 was higher in PD (0.67) than in controls (0.57) (Table 1). The association of SNP0070 was significant in genotype frequency, allele frequency, dominant model and recessive model. Of the two disease models, allele C of SNP0070 was more significantly associated in the recessive model than in the dominant model (Table 1).

Linkage disequilibrium (LD) mapping and search for susceptibility SNPs

We performed LD mapping in a 430 kb region around SNP0070. This region contains two genes: *SNCA* and *MMRN1*. Using SNP0070 and 28 additional SNPs in this region, we genotyped 134 control subjects and constructed an LD map based on pairwise D' and r^2 (Fig. 1) (Supplementary Material, Table S2). Three LD blocks were observed on the basis of D' ($D' > 0.9$). The entire *SNCA* gene was included in a block containing SNP0070 (block 2). The *MMRN1* gene was in another LD block, indicating that *MMRN1* does not correlate with the SNP0070 association (Fig. 2).

To search for the most strongly associated SNP(s) in the region, we next performed association studies with these 29 SNPs (Fig. 2; Table 2). We found significant associations for SNPs in block 2, but not in blocks 1 and 3. Block 2, thought to be a susceptibility block for PD, was further analyzed on the basis of r^2-values. Of the 19 SNPs in block 2, 16 belonged to three groups with high pairwise r^2 (>0.85) and the remaining three did not belong to any group (Fig. 1; Table 2) (Supplementary Material, Table S2). Six SNPs in group 1, including originally screened SNP0070 and five additional SNPs (0203, 0204, 0205, 0207 and 0209), showed prominent association with PD ($P = 2.0 \times 10^{-9}$–1.7×10^{-11}, allele 1 versus allele 2) (Fig. 2; Table 2). Population attributable risk (PAR) (22) of SNP0070 was 42.5% in the dominant model and 18.5% in the recessive model.

We next performed haplotype analysis using six representative SNPs in block 2 (Table 3). Six common haplotypes (>1% of PD and controls) covered >90% of the population haplotypes in both PD and controls. The major haplotypes 1 and 2 showed significant associations; however, their P-values were not lower than that of any single SNP in group 1. Therefore, the presence of hidden SNP(s) with a lower P-value than group 1 seemed unlikely, as was the possibility that the haplotype(s) is implicated in PD susceptibility. These findings establish the six SNPs in group 1 as the strongest susceptibility SNPs. All showed stronger associations in the recessive model than in the dominant model, similar to the originally screened SNP0070 (Table 4).

Taken together, our genetic analyses indicate that *SNCA* is a definite susceptibility gene for sporadic PD and that multiple SNPs in group 1 are susceptibility SNPs, likely in a recessive model.